PARTICULATE EMISSIONS FROM SELECTED COMBUSTION SOURCES AND THEIR PATHOLOGICAL IMPACTS ON THE LUNG TISSUES OF MALE ALBINO MICE

JOSEPHATE ONG'ERA BOSIRE

A Thesis Submitted to the Graduate School in Partial Fulfillment of the Requirements for the Award of the Degree of Master of Science in Chemistry of Egerton University

EGERTON UNIVERSITY

NOVEMBER, 2016

DECLARATION AND RECOMMENDATION

DECLARATION

This thesis is my original work and has not been presented either in part or wholly for the award of a degree in any institution.

Signature…….. Date……..

Josephate Ong'era Bosire

SM11/23526/14

RECOMMENDATION

This thesis has been submitted with our approval as supervisors according to Egerton University regulations.

Signature……. Date……

Dr. Joshua Kibet, Ph.D.
Egerton University

Signature……..… Date…….

Dr. Thomas Kinyanjui, Ph.D.
Egerton University

COPYRIGHT

DEDICATION

It is with sincere regards that I dedicate this work to my loving parents (Mr. David Bosire and Mrs. Mary Bosire), my siblings especially Brother Douglas and his family, my wife Prexiedes, and my daughter (Mary-Patience) who have blessed me with so many opportunities in life and allowed me to grow up and become myself.

ACKNOWLEDGEMENT

I give thanks to God for giving me sufficient grace to accomplish this task successfully. I acknowledge Egerton University for according me an opportunity to do my Msc in this institution. My sincere gratitude is dedicated to my supervisors, Dr. J. K. Kibet and Dr. T. Kinyanjui of Egerton University, for giving me the chance to undertake this study and ensuring that everything was done right during my entire period as a student at Egerton University. I am sincerely honoured to have been their student. My parents, brothers, sisters and friends are greatly acknowledged for their prayers, financial and moral support throughout this research. I thank Egerton University, especially the Departments of Chemistry and Biological for providing the necessary support and facilities towards the accomplishment of this study. Many thanks to the Dr. Kibet research group for always providing support and promoting a collaborative scientific environment especially Caren Kurgat, Nicholas Rono and Douglas Nyangoya. I also thank Dr. Ngure and Mr. Benson for their guidance in pathological studies. The Directorate of Research and Extension is acknowledged for partially funding this work. Finally, I would like to acknowledge Dr. Moses Langat and his team in the University of Surrey for providing critical support during the analysis of SEM and GC-MS samples.

ABSTRACT

Particulate emissions and organic volatiles produced by incomplete combustion processes have attracted the attention of many environmental experts. Consequently, increasing concern has been directed towards the study of human health problems caused by carcinogenic and mutagenic soot components such as polycyclic aromatic hydrocarbons (PAHs) and polyenes from various combustion systems. Soot from many combustion systems are well-known precursors for numerous toxicological impacts in the environment as well as biological structures. This study investigated the nature and toxicological effects of soot from simulated forest fire, vehicular exhaust, and tyre burning. Soot from these sources was trapped in the gas phase using gas trapping apparatus and then dissolved in dichloromethane through a porous tube diluter. Volatiles from soot were extracted in dichloromethane for analysis using Gas Chromatography interfaced with a Mass Spectrometer (GC-MS). The energetics of selected PAHs and their corresponding free radicals was explored using high level quantum chemical calculations. Accordingly, the Density Functional Theory (DFT/B3LYP) in conjunction with 6-31G basis set was used in this study. The size distribution analysis and surface morphology of soot was examined using a scanning electron microscopy (SEM). To simulate chronic environmental pollution, 12-week old male albino mice were exposed to particulate emissions at a rate of ~ 250 $\mu g^{-3} day^{-1}$ (measured by a gas flow meter) and their lung tissues were extracted for bioassay analyses. Comparisons were made between the lung tissues of mice exposed to the particulate emissions from the three sources, and the control mouse in order to determine the biological impact of particulates on the functioning of the lung tissues. Igor and Image *J* computational softwares were used to characterize micrograph images. Swelling and shrinking of lung tissue cells was observed as a result of exposure to tyre and diesel exhaust particulate emissions which caused disconnection of tissues and damage to the blood capillaries within the lung alveoli. Organic volatiles detected from tyre and diesel combustion included benzene, benzo[a]pyrene, anthracene, and cyclopentafused PAHs such as fluorene and fluoranthene. The average particulate size of emissions from simulated forest fire using SEM was found to be 11.51 ± 4.91 μm. This study has shown that most of the emissions from simulated forest fire fall under particulate matter of ≤10 μm in size. Simulated forest fire particulates caused minimum damage to the lung tissues whereas particulate emissions from diesel and tyre caused grave damage to the lung system of the mice. These effects may be attributed to toxic organic volatiles as well as particulates which carry with them active radicals and toxic organic intermediates into the respiratory system.

TABLE OF CONTENTS

DECLARATION AND RECOMMENDATION ..... **ii**

COPYRIGHT ..... **iii**

DEDICATION ..... **iv**

ACKNOWLEDGEMENT ..... **v**

ABSTRACT ..... **vi**

LIST OF TABLES ..... **x**

LIST OF FIGURES ..... **xi**

LIST OF SCHEMES ..... **xii**

LIST OF APPENDICES ..... **xiii**

LIST OF ABBREVIATIONS AND ACRONYMS ..... **xiv**

CHAPTER ONE **1**

INTRODUCTION **1**

1.1 Background information 1

1.2 Statement of the problem 4

1.3 Objectives 4

1.3.1 General objective 4

1.3.2 Specific objectives 4

1.4 Hypotheses 5

1.5 Justification 5

CHAPTER TWO **6**

LITERATURE REVIEW **6**

2.1 Sources of soot 6

2.2 Formation of soot in the gas-phase 8

2.2.1 Soot particle precursors 8

2.2.2 Growth of aromatics 9

2.2.3 Growth of other species 10

2.2.4 Migration reactions 11
2.2.5 Surface migration 12
2.3 Particulate phase 13
2.3.1 Particle nucleation 13
2.3.2 Particle coagulation 14
2.3.3 Soot particle oxidation 15
2.4 Histopathology of particulate emissions 16
2.5 The toxicological impacts of soot 17
2.6 Visibility and skin irritation 18
2.7 Odour 18
2.8 Soiling and damage to materials 18
2.9 Significance of this study 19
CHAPTER THREE 21
MATERIALS AND METHODS 21
3.1 Materials 21
3.2 The reactor 21
3.2 Collection of soot from forest fire simulation 22
3.3 Particulate emissions from the thermal degradation of waste tyre 23
3.4 Soot collection from vehicular exhaust 23
3.5 Gas Chromatography-Mass Spectrometer (GC-MS) Analysis 23
3.6 Scanning Electron Microscopy (SEM) analysis 24
3.7 Computational methodology 24
3.8 Experiments involving research mice 24
3.8.1 Mice handling 24
3.8.2 Soot exposure protocol for albino mice 25
3.8.3 Mice respiratory tissue analysis 25
3.9 Data analysis and presentation 26

CHAPTER FOUR **27**

RESULTS AND DISCUSSION **27**

4.1 Molecular distribution of organic volatiles from selected combustion sources 27

4.2 Molecular volatiles from simulated forest fire 27

4.3 Molecular toxins Emission from Tyre and Diesel 29

4.4 Oxygenated organic volatiles 33

4.5 Molecular toxins that may easily transform into hazardous products 34

4.6 Decomposition profile of waste tyre 35

4.7 Characterization of soot organic volatiles from fuel combustion 36

4.8 Statistical analysis of particulates 38

4.9 Environmental and biological health effects of molecular volatiles 38

4.10 Computational results 40

4.11: Molecular orbitals and electron density maps 42

4.12 Histochemistry 45

4.12.1 Examination of lung damage by particulate matter 45

4.12.2 Effects of particulate emissions on the lungs tissues of albino mice 47

CHAPTER FIVE **50**

CONCLUSIONS AND RECOMMENDATIONS **50**

5.1 Conclusion 50

5.2 Recommendations 51

REFERENCES **52**

APPENDICES **67**

LIST OF TABLES

Table 4.1: Volatile components from simulated forest fire identified using GC-MS……..…28

Table 4.2: Organic volatiles from the thermal degradation of diesel sample…….…….30

Table 4.3: Organic volatiles from the thermal degradation of tyre……..…...32

Table4.4: Mean sizes of particulates formed during tyre combustion and simulated forest fire…….39

Table 4.5: Band-gap energies for the PAHs investigated in this work……...4

LIST OF FIGURES

Figure 2.1: Examples of PAHs; naphthalene and acenapthalene…..7

Figure 3.1: Simulation in the reactor……...21

Figure 3.2: Reactor assembly and the tyre gas-phase trapping apparatus……...22

Figure 4.1: GC-MS chromatogram for selected volatiles from forest fire……..27

Figure 4.2: GC-MS chromatogram for selected volatiles from diesel combustion……....30

Figure 4.3: GC-MS chromatogram for selected volatiles from tyre combustion……....32

Figure 4.4: Oxygenated volatiles detected in this study……..34

Figure 4.5: Benzofuran like structures of some molecular compounds identified in this work…….……..35

Figure 4.6: Char percentage (%) yield from thermal degradation of tyre……...35

Figure 4.7: SEM image and particle size distribution (Gaussian red) of soot particles from simulated forest fire…….……..36

Figure 4.8: SEM image and particle size distribution (Gaussian blue) of soot particles from tyre burning…….……..37

Figure 4.9: The HOMO-LUMO band gap for fluorene determined using Chemissian…..…43

Figure 4.10: 2-D electron density contour map for fluorene calculated using Chemissian……44

Figure 4.11: 3-D molecular orbital diagram showing electronic density for fluorene at an isovalue of 0.02…….…44

Figure 4.12: 1 is the lung exposed to diesel while **2** is the lung exposed to tyre particulates……....45

Figure 4.13: Lung tissue photographs obtained from a light microscope at ×200 magnification ……...….46

LIST OF SCHEMES

Scheme 2.1: Mechanistic formation of soot from biphenyl radical…….……....10

Scheme 2.2: Mechanistic formation of soot via acetylene pathway……....10

Scheme 2.3: The formation of a cyclopentadiene precursor for soot formation…….....11

Scheme 2.4: Interconversion of five- and six-membered rings……..…….11

Scheme 2.5: Migration of the cyclopenta ring along zigzag aromatic edges……..11

Scheme 2.6: Mechanistic formation of soot via surface migration of radical species……....13

Scheme 2.7: Soot nucleation……...14

Scheme 4.1: Formation of α-octadecenyl radical (carbon-centered radical) from molecular α-octadecene…….37

Scheme4.2: Mechanistic formation of oxygen centered radicals from methoxy acetic acid……...…….40

Scheme4.3: Proposed mechanism for the conversion of molecular 1, 2-benzene dicarboxylic acid to isobenzofuran-1, 3-dione and bicyclo [4.1.0] hepta-1, 3, 5-trien-7-one.....…...41

LIST OF APPENDICES

Appendix 1: A sample of SEM micrograph from tyre burning……..67

Appendix 2A: MS-Fragmentation pattern for benzene……...68

Appendix 2B: MS-Fragmentation pattern for fluorene……...69

Appendix 2C: MS-Fragmentation pattern for anthracene……...……70

Appendix 2D: MS-Fragmentation pattern for fluoranthene……..……..71

Appendix 2E: MS-Fragmentation pattern for benzo[a]pyrene……...……72

Appendix 3: Thermochemistry output file for optimization of isobenzofuran-1, 3-dione…….……73

Appendix 4A: 2-D electron density contour map for fluoranthene predicted using Chemissian……...……75

Appendix 4B: HOMO-LUMO band gap for fluoranthene determined using Chemissian……...76

Appendix 5: Albino mice in the cage for soot/smoke exposure…….……77

LIST OF ABBREVIATIONS AND ACRONYMS

ANOVA	Analysis of variance
DCM	Dichloromethane
DE	Diesel exhaust
DFT	Density Function Theory
GC-MS	Gas chromatography interfaced with Mass spectrometer
HACA	Hydrogen-Abstraction-Acetylene(C)-Addition
HCl	Hydrochloric acid
HOMO	Highest Occupied Molecular Orbital
HPLC	High Performance Liquid Chromatography
IARC	International Agency for Research on Cancer
KEMRI	Kenya Medical Research Institute
LUMO	Lowest Unoccupied Molecular Orbital
NIST	National Institute of Standards and Technology
nm	Nanometer
OSHA	Occupational Exposure Safety and Health Administration
Oxy-PAHs	Oxygenated polycyclic aromatic hydrocarbons
PAHs	Polycyclic aromatic hydrocarbons
PM	Particulate matter
$PM_{2.5}$	Refers to particles with a diameter of less than 2.5 microns
PM_{10}	Refers to particles with a diameter less than 10 microns but greater than 2.5 microns
$PM_{0.1}$	Refers to particles with a diameter less than 0.1 microns
SEM	Scanning electron microscopy

CHAPTER ONE

INTRODUCTION

1.1 Background information

The principal focus of this investigation was to examine the respiratory injury on the lung tissues of male albino mice as a result of exposure to particulate emissions (soot) and organic volatiles from various combustion sources. Generally, particulate matter is defined as an aggregate of small particulates, liquid droplets, and vapors that have been associated with respiratory and cardiovascular morbidity, and mortality in susceptible populations (Lippmann and Schlesinger, 2000). Ambient particulate matter (PM) of various particle dimensions from different sources has been found to originate from a number of human activities (i.e. tyre burning, diesel combustion and forest fires) and natural sources (Kelly and Fussell, 2012). During incomplete combustion in air-limited conditions at moderately high temperatures, PM emissions are dominated by solid carbon aggregates (soot) (Gwaze *et al.*, 2006). The health effects of inhaled particles and organic toxins are highly dependent on the deposition and retention of particles in the lung (Kreyling *et al.*, 2006). The deposition possibility and deposition site of particles is not only governed by their aerodynamic characteristics, such as size, density, and shape, but also by other physicochemical properties such as hygroscopicity (i.e. water uptake) (Bølling *et al.*, 2009). Experimental studies have suggested a range of physicochemical properties influencing the toxic and inflammatory potential of PM and possibly particle-induced health effects (Schwarze *et al.*, 2006). Additionally, soot particulates are involved in the transmission of nasty odours. For instance, odours from incinerators, open fires and burning of food products are transmitted by particulate emissions (Köhler and Allgeier, 2015).

Histochemistry as the aspect of histology concerned with the identification of chemical components in biological cells and tissues has been used to explain more about soot effects in body organs (Vohr, 2016). To understand the impacts of particulate emissions in biological systems, there exist two major components to be analyzed; the first and most clinically important are the physiological changes that occur and must be managed clinically to obtain optimum outcomes (Bates *et al.*, 2015). The second component relates to the biochemical changes responsible for the observed physiological changes (Bergethon, 2013). Consequently, histochemistry evaluates the soot emissions as an altering agent in the microstructures of the biological cells (Fahlman, 2011). To appreciate the impacts of soot on

biological structures, microscopy techniques such scanning electron microscopy (SEM), the electron microscope, and the light microscope were used in this study.

Particulate emissions from combustion of tyre, diesel, and other petroleum fuels is a dominant contributor to particulates of ≤ 2.5 μm ($PM_{2.5}$) and particulates of ≤ 10 μm (PM_{10}) and contains emissions of carbonaceous particles with fused and free polycyclic aromatic hydrocarbons (PAHs) (Xi and Zhong, 2006). These fuels may generate long chain hydrocarbons which further undergo degradation to produce free radicals which are considered biologically hazardous. PAH and long chain hydrocarbons metabolism in the body generates electrophilic and reactive metabolites that have been indicated as initiators of pulmonary cytochrome P450 in diesel exhaust particles (Murphy *et al.*, 2008). Furthermore, ambient airborne particulates consist of persistent free radicals and reactive oxygen species (ROS) implicated in the generation of cellular oxidative stress and cell damage (Li *et al.*, 2008). The persistent oxidative stress contributes to decreased lung function and exacerbates asthma, bronchitis, and pneumonia among people living in areas of high levels of particulate air pollution (Perez-Padilla *et al.*, 2010; Ko and Hui, 2012). Although exposure to particulate emissions has been linked to diminished lung development and function in children, the underlying biological mechanism responsible for enhanced susceptibility is largely unknown (Jayaraman *et al.*, 2010).

Epidemiological studies have shown that there is an association between ambient air PM concentrations and health effects. PM, in general, has been mostly linked to excess cardiovascular mortality (Brunekreef and Forsberg, 2005), lung cancer (Sexton *et al.*, 2007; O'Connor *et al.*, 2008) and cardiac arrhythmias (Delfino *et al.*, 2005). All these effects vary in strength with sampling location, type, and season and fraction size. Nonetheless, granular particulates have been mostly associated with respiratory disease and cardiopulmonary morbidity (Brunekreef and Forsberg, 2005; Brook *et al.*, 2010). Toxicological research has confirmed the organic credibility of the findings of epidemiology studies and demonstrated that PM-induced toxic effects are often dependent upon PM size and composition (Mirowsky *et al.*, 2013). Moreover, if the origin of the smoke particulate emissions is of organic nature, then the smoke may cause numerous ill health problems including central nervous system breakdown, lung inflammation, and mucous membrane irritation in addition to other ailments (Chaturvedi, 2010). The oxidative potential of airborne particles is yet to be understood; however, some studies have established that fine PM have been associated with the generation of high levels of reactive oxygen species (Bates *et al.*, 2015).

Soot is the mass accumulation of polycyclic aromatic hydrocarbons (PAHs) species above a certain size i.e. transition from gaseous species to solid particles through chemical growth (Frenklach *et al.*, 1985; Frenklach and Wang, 1991, 1994b). Soot can also be considered as a product of incomplete combustion, accompanied by the presence of PAHs, nano-sized carbon particles and few fullerenes (Bachmann *et al.*, 1996; Bruno *et al.*, 2002; Apicella *et al.*, 2006). Soot formation comprise four major processes i.e. homogeneous nucleation of soot particles, particle coagulation, particle surface reaction (growth and oxidation), and particle agglomeration (Palmer and Cullis, 1965). Although soot formation is a complex area of study, it has become necessary to investigate various phenomena at the nano scale and how it affects biological functions as precursors for cancer, oxidation stress, aging, and other degenerative diseases that affect the respiratory landscape. Chronic exposure can lead to allergies, bronchitis, and emphysema, while acute exposure can cause impaired judgment, eye and respiratory irritation, and even death. Particulate soot is a major cause of reduced visibility in many parts of the United States. It can also cause damage to paints and building materials (Berdahl *et al.*, 2008).

The physics of soot formation is a fire which is a consequence of a fuel among other conditions. Therefore, heat, fuel, and chemical reaction are necessary components for the development of a fire (Chaturvedi, 2010). Fire is a complex, dynamic, and physicochemical processes and is the result of rapid chemical reaction generating soot, heat, flame, and light (Lautenberger *et al.*, 2005). Soot consists of PM, as well as a variety of invisible combustion gases and vapours suspended in the fire atmosphere (Gad, 1990; Wright *et al.*, 2009). Particulate matter is the sum of all solid and liquid particles both organic and inorganic particles such as soot, dust, smoke and liquid droplets (Silverman, 2012). These particles vary greatly in size, composition and origin. Based on the size, particulate matter is often divided into two groups i.e. the coarse fraction that contains larger particles with a size ranging from 2.5 µm to 10µm ($PM_{2.5}$ – PM_{10}) and the fine fraction contains the smaller ones with a size up to 2.5 µm ($PM_{2.5}$) (Marcazzan *et al.*, 2001). The particles in the fine fraction which are smaller than 0.1 µm are called ultrafine particles.

Accordingly, this study examines particulates, organic volatiles, and the health impacts of particulate emissions from various sources on the lung tissues of male albino mice with the aim of deriving the pathological impacts of inhaling such particulates by higher-order animals such as man. This contribution is also necessary in understanding the health consequences of airborne particulates and organic toxins especially from vehicular soot, indiscriminate tyre

burning, and disasters such as fireworks and forest fires. The information obtained is fundamental in assisting governments and environmentalists to make informed decisions concerning environmental pollution from the thermal degradation of organic materials. Generally, the organic volatiles (PAHs) considered detrimental to biological health has been discussed extensively in this study.

1.2 Statement of the problem

In view of increased forest fires, increased vehicular emissions and unconventional thermal destruction of tyres, soot and organic pollutants have gained significant attention in biological and environmental health. Soot has been reported to contain substances that are not only carcinogenic but also mutagenic. They act as precursors for oxidative stress, cancers and respiratory problems. Previous studies have shown that soot can cause decreased lung function, heart and liver problems. Soot particulates exists in the environment in form of PAHs, polyenes, coronene and long chain hydrocarbons. According to a major study published in New England Journal of Medicine in 2007, long term exposure to urban air pollution containing soot increases the risk of coronary heart diseases. In several human experimental studies using a well-validated exposure chamber setup, diesel exhaust (DE) has been linked to acute vascular dysfunction, respiratory problems and increased thrombus formation.

1.3 Objectives

1.3.1 General objective

To investigate soot particulate emissions from various combustion sources and their pathological impacts on the lung tissues of albino mice

1.3.2 Specific objectives

1. To determine the molecular combustion by-products from the thermal degradation of various biomass materials (tyre, diesel, and simulated forest components).
2. To characterize the particulate emissions (soot) from various combustion sources.
3. To explore the physiological effects of various particulate emissions on the respiratory tissues of male albino mice.

1.4 Hypotheses

1. The thermal degradation of selected biomass materials will not give similar molecular reaction products

2. Several combustion sources will not emit particulates of the same aerodynamic diameter

3. Soot will not cause lethal physiological consequences on the respiratory tissues of male albino mice

1.5 Justification

The mechanism by which particulate emissions and organic volatiles cause toxicity is quite complex. In the past few years, significant effort has been made towards understanding the particulate nature of soot from various combustion systems and their toxicological impacts in biological structures. Despite soot formation being a complex study area, it has become necessary to investigate their particulate size and their clinical effects on human health and natural ecosystems. Traffic emission studies suggest increased rates of respiratory and cardiovascular disease and risk of premature death near busy urban streets or highways. Therefore, great attention has been drawn to the chemistry of particulate emissions, PAHs and hydrocarbons such as 1, 3-butadiene, benzene, and toluene by scientists all over the world. Accordingly, the chemistry of rich flames, particularly that involved with hydrocarbon growth into PAHs and ultimately soot, has become one of the most active research areas in combustion chemistry. Furthermore, the histochemistry of soot has gained mounting global attention through the use of research animals.

CHAPTER TWO

LITERATURE REVIEW

2.1 Sources of soot

Soot formation is understood to have two major patterns in the combustion processes (Indarto, 2008). The first and probably the most famous formation of soot is through aggregation of poly-cyclic aromatic hydrocarbons (PAHs) (Bauschlicher *et al.*, 2000). This is also known as "growing PAHs" scheme in which the precursors (e.g. ethylene or small hydrocarbons radical) react to form cyclic molecules such as benzene (C_6H_6), naphthalene, or coronene (Norinaga and Deutschmann, 2007). Emissions from the selected combustion sources are major concern due to hazardous gases such as CO and SO_2, polycyclic aromatic hydrocarbons (PAH) and particulate matter that are produced from carbon, sulfur and other components used in tyre and diesel production. A recent research conducted by Downard *et al.* (2015) revealed that emissions of hydrocarbons ranged between 1800-60,000, 31,000-35,000 and 1300- 3700 $mgkg^{-1}$ of tyre burned, respectively during a controlled burn study. The total average emissions ranged from 64,500-149,000 $mgkg^{-1}$ of tyre in an open burning simulation (Downard *et al.*, 2015).

Poly-cyclic aromatic hydrocarbons (PAH) are major class products of combustion of tyre and diesel. The formation of PAHs and soot has become one of the central themes of research activities in the area of combustion of hydrocarbons fuel and other materials such as biomass and municipal waste incineration (Paulik *et al.*, 2016). Various theoretical models simulate particle formation and evolution in different types of flames; however, soot formation modeling in terms of short time scales, for example the shock tube experiments, takes place in a few milliseconds. This restriction has made it difficult to model soot formation with the use of the conventional Hydrogen-Abstraction-Acetylene-Addition (HACA) model (McIntosh and Russell, 2014). It requires the investigation and the development of various chemical reaction routes of soot precursor formation and growth together with an adequate kinetic representation. This is because of the mounting environmental concerns of pollutant emission from combustion sources and fires. For this reason, research activities span experimental, theoretical and computation efforts, and covers a diverse spectrum of the physics and chemistry of the combustion processes such as; homogeneous nucleation of soot

particles, particle surface growth and oxidation, particle coagulation and agglomeration (Eggersdorfer and Pratsinis, 2013).

A study that was conducted in a laboratory environment showed that emission factor for total (gaseous and particulate) PAH was 5330 $mgkg^{-1}$ of worn out tyre in an open burning simulation and 11,450 $mgkg^{-1}$ of powdered tyre in a controlled thermal degradation study (Orasche *et al.*, 2012). PAHs are primary and secondary reaction products from combustion of tyre. At higher temperatures in controlled environments, it has been found that light olefinic and aromatic compounds, arising from butadiene and styrene, are volatilized. These volatilized light olefins and aromatics evolved eventually combines to form PAH compounds via Diels-Alder type reactions (Saunders, 2013). The PAHs produced especially, from tyre and diesel combustion range from two to six rings in size and may contain methyl or other alkyl substituents. The major component of tyre combustion emissions is benzo[a]pyrene (B[a] P). This is a five-ring PAH that has been extensively studied as it is very toxic and it has been classified by the International Agency for Research on Cancer (IARC) as a known human carcinogen and is used as a general indicator of carcinogenic PAH emissions (Tilton *et al.*, 2015). In oxygen limited combustion environments, PAH emissions increase. Quantities of PAH emissions from large-scale open burning of tyres are limited, since these PAH emissions have been studied under controlled environments (Siddens *et al.*, 2012). Examination of soot and liquid samples collected from tyre combustion in Quebec revealed 165 individual PAH with two to seven aromatic rings and molecular weights ranging between 216 to 302 Daltons (Da). Aromatic compounds containing sulfur, nitrogen and oxygen, including phenols, quinolines, thiophenes and carbazoles have also been identified as products of tyre combustion (Wang *et al.*, 2007). Some examples of PAHs are presented in Figure 2.1.

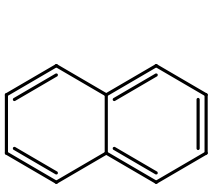

naphthalene

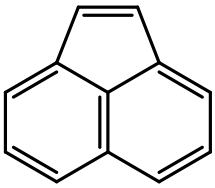

acenaphthalene

Figure 2.1: Examples of PAHs; naphthalene and acenapthalene.

Along with the above properties, PAHs also have the ability to travel long distances in the environment. PAHs, especially those with three to four rings, are semi-volatile and have the

ability to screen between gaseous and particulate phases. Moreover, PAHs can bond on surface waters and soils for long periods of time, which later are then re-evaporated into the atmosphere. PAHs are also strongly associated with soot or black carbon that is released during fossil fuel combustion (Weidemann *et al.*, 2016).

Recent research has also shown that PAHs can react with particles and sunlight once emitted or exposed to the environment. These reactions can alter the behaviour of the chemicals, or transform them into new toxins. Once in the atmosphere, PAHs can react with other pollutants such as ozone, hydroxyl radical, sulfur dioxide, and nitrogen dioxide. Upon reacting with these chemicals, PAHs can become more toxic (Abdel-Shafy and Mansour, 2016). Some PAHs have been shown to have half-lives of just hours to days in the atmosphere due to these chemical transformations (Forbes and Garland, 2016).

Another method of soot formation is via polyene molecules ($C_{2n}H_n$) (Crittenden and Long, 1973). This scheme is rarely addressed, although polyenes have been detected in high concentrations during combustion processes (Mansurov, 2005). Therefore, polyenes could be one of the major precursors for soot formation in combustion systems due to their unique reactivity. A detailed kinetic model for the formation of soot from the perspective of flame modeling can be viewed as comprising of two principal components: gas-phase chemistry, which determines the flame structure, and soot particle dynamics, which describes the evolution of the particle ensemble.

2.2 Formation of soot in the gas-phase

The mechanism of soot formation consists of several stages. For instance, starting with an aliphatic fuel, the fuel molecules are first broken down into smaller hydrocarbon molecules and free radicals either by pyrolysis or oxidation reactions. These small particles exist in the gaseous form which latter combine to form larger particles.

2.2.1 Soot particle precursors

The nature of soot particle inception involves polyacetylenes (polyenes), iron species, or polycyclic aromatic hydrocarbons as the key gaseous precursors to soot formation (Calcote, 1981). Polyenes ($C_{2n}H_2$) can be described as a linear molecule consisting of carbon atoms and, in the neutral charge state; they have one hydrogen atoms in each end of the chain (Kugler, 1999). The highest detected polyenes molecule in the flame was as long as $C_{14}H_2$,

but only C_4H_2 can be isolated in significant amounts (Gaffney *et al.*, 2015). Polyene concentration was varied depending on the fuel used for the combustion and the reaction time. The idea of polyene as the soot growing precursor was proposed by Homann (1967) who found that there were a group of species which disappeared rapidly during the soot growth and were no longer detected at the end of the oxidation reaction zone (Mansurov, 2005; Indarto, 2009). From another experimental work, it was pointed out that the investigation of the absorption profiles for 'pre-soot' species in pyrolysis and oxidation of different fuels indicated the presence of species capable of absorbing in the visible and ultraviolet region of the spectrum before the emergence of soot (Haynes, 1981). However, the major sources of soot particles is via macro-cycloalkanes and PAHs (Kamens *et al.*, 1988). The PAHs hypothesis also embraces the particle inception through formation of aromatic-aliphatic-linked hydrocarbons which later graphitize (D'Anna *et al.*, 1994). The formation and growth of aromatic species bridges the main combustion zone chemistry and soot formation. The aromatic molecules are themselves toxic and subject to environment regulations (Shaw and Connell, 1994).

2.2.2 Growth of aromatics

The modeling of soot formation and growth in combustion was considerably influenced by the work of Frenklach (Frenklach *et al.*, 1985; Frenklach and Wang, 1994a). The authors suggested a detailed kinetic mechanism of soot formation and growth via PAHs called HACA. This model involves Hydrogen-Abstraction-Acetylene-Addition (HACA) which has two principal steps i.e. abstraction of a hydrogen atom from the reacting hydrocarbon by a gaseous hydrogen atom which activates the aromatic molecule (Frenklach and Wang, 1991).

$$A_i + H \rightarrow A_{i\text{-}} + H_2 \qquad (2.1)$$

Equations 2.1 and 2.2 shows the addition of gaseous acetylene molecule to the radical site formed which propagates molecular growth and cyclization (D'Anna *et al.*, 1994).

$$A_{i-} + C_2H_2 \rightarrow products \qquad (2.2)$$

A_i is an aromatic molecule with i peri-condensed rings and $A_{i\text{-}}$ is its radical. The significance of these two reaction-paths feature was identified in the very first attempt at numerical modeling of detailed reaction kinetics of the growth of aromatics (Frenklach *et al.*, 1985) . The first step activates a molecule to further growth by converting it to a radical. Therefore, the key feature of this step (HACA step), as proposed in equations 2.3 and 2.4 is its reversibility (Frenklach and Warnatz, 1987; Richter *et al.*, 2005) i.e.

$$A_{i-} + H_2 \rightarrow A_i + H \quad (2.3)$$

$$A_{i-} + H_2 \rightarrow A_i \quad (2.4)$$

The reversibility of the acetylene addition step, reaction (2.4), or more precisely, the degree of its reversibility is what determines whether this step will contribute to molecular growth (Siegmann, 2002). Kinetic model of soot formation, from the perspective of flame modeling can be viewed as a composition of two principal components; gas-phase chemistry, which determines the flame structure, and soot particle dynamics, which describes the evolution of the particle ensemble (Chung, 2011).

2.2.3 Growth of other species

Acetylene is not the only species that propagates the growth of aromatic rings, but also methyl, propargyl, and cyclopentadienyl (Henning and Howard, 2000). According to Glassma (1979) stabilized structure of the reacting radicals of hydrocarbons with conjugated structure and their derivatives are critical intermediate to soot nucleation (Frenklach *et al.*, 1983). For instance, in the pyrolysis of benzene, the aromatic growth is initiated by the formation of biphenyl as presented in scheme 2.1 (Perez *et al.*, 1991).

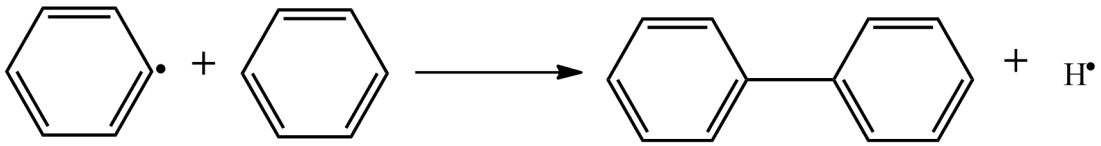

Scheme 2.1: Mechanistic formation of soot from biphenyl radical

Scheme 2.2 proposes the growth of soot via acetylene addition according to Frenklach, (1986 and 1988). This pattern appears at different conditions and fuel as well as in flames with increased stoichiometry and pressure (Kazakov *et al.*, 1995).

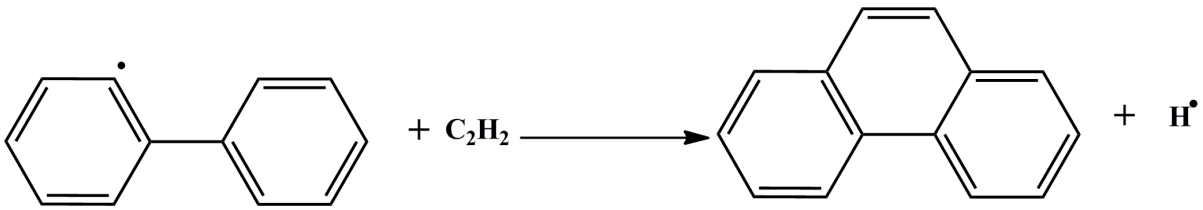

Scheme 2.2: Mechanistic formation of soot via acetylene pathway

2.2.4 Migration reactions

Theoretical investigations reveal new reaction pathways for aromatic ring growth (Richter and Howard, 2000). For instance the formation of soot via a five-membered aromatic ring as shown in scheme 2.3, anchors this theory.

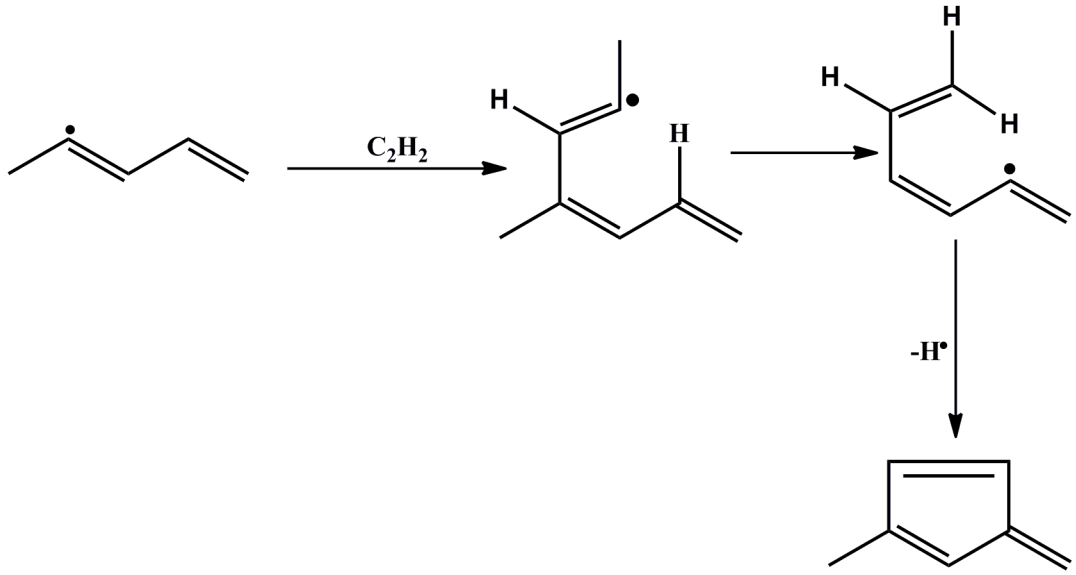

Scheme 2.3: The formation of a cyclopentadiene precursor for soot formation

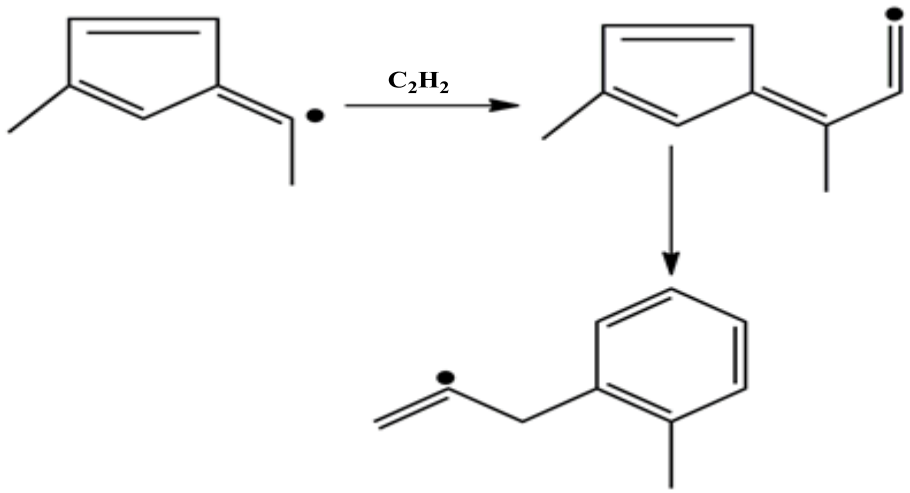

Scheme 2.4; Interconversion of five- and six-membered rings

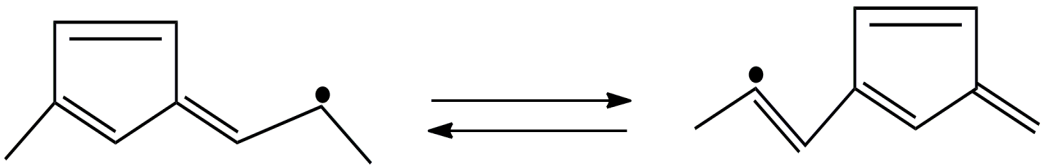

Scheme 2.5: Migration of the cyclopenta ring along zigzag aromatic edges

All the pathways above have one critical mechanistic feature in common in that the reaction pathway is induced or assisted by hydrogen atom migration (Frenklach., 1998). For large aromatic structures, like condensed multi-ring soot precursors or those developed at the edges of the soot particle surface, the H migration step opens an additional and somewhat faster channel for reaction pathways 2.3, with the result of at least doubling the rate of cyclization. Reaction pathway for instance, 2.4 and 2.5 open substantially new possibilities for surface growth, as will be discussed in the next section. Researchers have studied the five-member ring migration along a graphene edge and concluded that an important implication of the migration phenomenon is that, while five-member rings are constantly being formed on the growing edge, they do not accumulate, but rather they are converted to six-member rings (Singh *et al.*, 2015).

2.2.5 Surface migration

The postulate of chemical similarity provides a natural extension of the gas-phase chemistry of aromatics, which in turn enables a faultless coupling of the gas-phase reaction model with that of surface growth and oxidation (Frenklach and Wang, 1994b). At the same time one must realize that the postulate of chemical similarity is only an assumption. In reality, one should predict differences between gaseous and surface reactions even in cases of seemingly analogous molecular interactions (Frenklach and Ping, 2004). The primary cause of the possible dissimilarity is the difference in steric confinements of reactive sites. In other words, the reaction of a gaseous species with a surface radical may have the ‘‘sticking probability ’’ and equilibrium constant varying with the nature of the neighbouring sites and their occupancy (May *et al.*, 2010). This phenomenon is presented in Figure 2.6. Furthermore, while the localized steric factors may affect the surface kinetics in its own right, sometimes, like in the case of surface migration, it leads to substantially different overall reaction kinetic patterns (Veshikini *et al.*, 2015). By analogy with diamond film growth, the five-membered ring migration has important implications for the surface growth of soot particles (Frenklach and Ping, 2004). The migrating five-membered rings will propagate the zipper filling of the zigzag surface, via the reaction pathway ensuring that the growth proceeds via a continuous front (Edwards *et al.*, 2014). A ‘‘collision’’ of these propagating fronts may create a site that cannot be filled by cyclization and thus cannot support further growth, again reminiscent of the diamond case (Frenklach, 2002). Formation of such surface defects may be responsible for the loss of reactivity of the soot particle surface to growth (Jorg *et al.*, 2000).

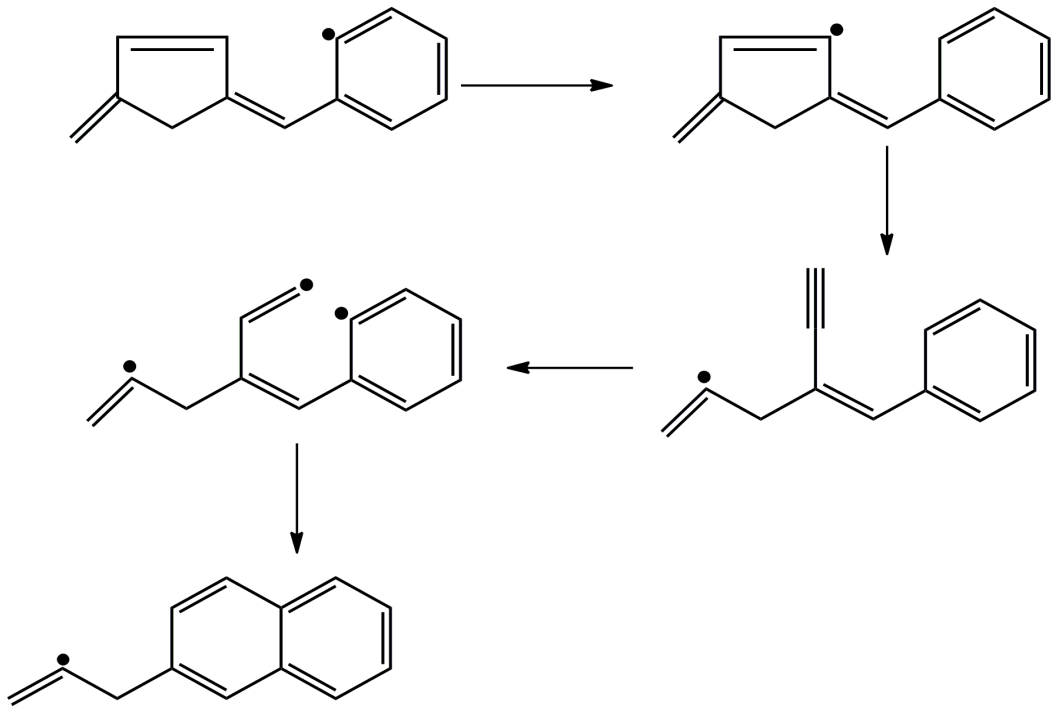

Scheme 2.6: Mechanistic formation of soot via surface migration of radical species

2.3 Particulate phase

In spite of the great effort in understanding the mechanism of hydrocarbons and soot formation, there are still numerous uncertainties which need to be studied experimentally and theoretically. The formation and evolution of soot particles includes processes like soot particle nucleation, surface growth and oxidation, coagulation and agglomeration which are briefly described in the following sections.

2.3.1 Particle nucleation

The transition of gas-phase species to solid particles is probably the least understood part of soot formation. Here, at some critical size of hydrocarbon radical species begin sticking to each other during collision, thus forming dimers (Frenklach and Wang, 1994b). PAH dimers collide with PAH molecules forming PAH trimers, or with other dimers to form tetramers, and so on. Individual PAH species keep increasing in size via molecular chemical growth reactions leading to soot formation (Frenklach *et al.*, 1985). To test for PAH dimerization and chemical-reaction growth of aromatics it was found that particles increasing in size were continually formed (Miller, 1991). However, a model of purely chemical growth for the soot nuclei formation has been suggested in a series of studies (Dobbins and Subramaniasivam, 1994). In this proposition, soot particles stick together to form chain-like structures (Chen *et*

al., 2010) as observed in scheme 2.7. Experimental data shows that this process occurs later when soot particles "mature" or "age" (Bejaoui *et al.*, 2015). The chain-like structure has been analyzed in terms of fractal geometry (Megaridis and Dibbins, 1990; Koylu and Faeth, 1992; Puri *et al.*, 1993). The possible pathway of soot nucleation according to Krestinin (1998) is as follows.

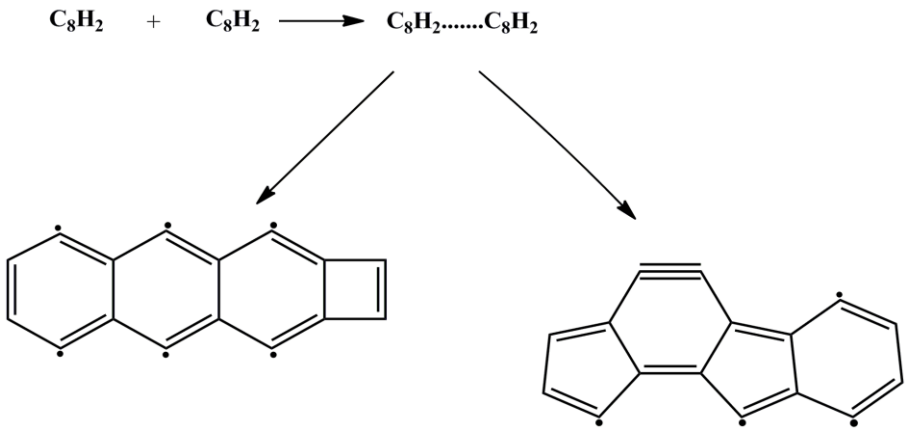

Scheme 2.7: Soot nucleation

2.3.2 Particle coagulation

This is a process in which small particles collide with each other and coalesce completely to larger spherical particles (soot). Experimental studies have shown that the particles in the initial stages of soot formation look spherical and later acquire a fractal shape (Haynes, 1981). Thus, particle coagulation is usually classified as coalescent growth and agglomeration into fractal aggregates (Mehta, 2008). In coalescent growth particles are assumed to be spherical. They collide and coalesce completely, forming new spherical particles (Gelbard and Seinfeld, 1980; Friedlander, 2000).

The experimental evidence (Dobbins and Subramaniasivam, 1994) and computational results show that there is a substantial deviation of particle size distribution function from self-preserving form in the soot particle inception zone (Frenklach and Wang, 1994b).

It is usually proposed that formation of spherical soot particles precedes that of aggregates, but the transition from spherical to fractal growth is not well understood (Appel *et al.*, 2000). According to Saarikoski *et al.* (2008) the particles are composed of viscous matter (liquid droplets) that coalesce completely at small size, but do not have sufficient time for fusion as the particle size increases (Saarikoski *et al.*, 2008). Also it has been shown that nearly spherical shape of the primary particle is the product of simultaneously occurring coagulation

and surface growth and that the transition to aggregates is caused by cessation of surface growth (Howard and Longwell, 1983). However, recent numerical simulations indicates that soot particle growth has been modeled using time-dependent Monte Carlo simulations via ensemble collisions between small geometrically perfect spheres (Khosousi and Benjamin, 2015; Liu *et al.*, 2015; Reddy *et al.*, 2015). This atomistic model for particle inception is a combination of kinetic *Monte-Carlo* and molecular dynamic methods. The model is applied to investigate the growth of aromatic compounds up to the nano-size range in chemically specific way. This approach preserves the atomic scale structures like bonds, bond angles and dihedral angles as the soot precursors evolve into three-dimensional structures (Violi, 2004). Consequently, with the collisions, the particle sphere surfaces grow at a prescribed rate (Zhang *et al.*, 2009). Through simulations, particle sphericity is affected by two factors; surface growth rate and size of the colliding particles (Yapp and Kraft, 2013; Khosousi and Benjamin, 2015).

2.3.3 Soot particle oxidation

The process of soot particle oxidation is similar to the surface growth. In fact, oxidation is also a surface reaction, in which primarily should be treated as catalytic combustion. Potential soot oxidants are O, O_2, OH, and CO_2. According to Frenklach (1987), the major oxidation process occurs at the very beginning of soot particle growth, which is the soot particle nucleation period, where a rapidly decreasing concentration of O_2 in fuel-rich environments is observed. However, the hydroxyl radical is the most abundant oxidizing species under fuel-rich condition. The authors stated that OH could suppress soot formation via oxidative destruction of precursors, and OH radical concentration might be an important factor in soot precursor kinetics (Higgins *et al.*, 2002). This led to a conclusion that OH radical is the limiting oxidative reactant under fuel-rich condition as the soot decreases with an increase in OH concentration. Experimental studies performed showed that CO_2 has chemical dilution, and thermal effects on soot formation reduction (Liu. *et al.*, 2001). They suggested that the chemical mechanism of CO_2 addition might be to promote the concentrations of oxygen atom and hydroxyl that in return increase the oxidation of soot precursors in soot formation regions. The researchers also observed that the concentration of acetylene decreases as a result of CO_2 addition. However, due to the lack of data on the mechanism of soot particle oxidation, a one-step treatment is often used, assuming the rate law for the CO formed as given by Warnatz *et al.* (2006).

$$\frac{d[CO]}{dt} = Y_i \cdot Z_i \cdot a_s \qquad (2.5)$$

where i =O, OH, O_2, Y_i = reaction probability when molecule i hits the soot surface, Z_i= collision number of molecule i per unit time and area, and a_s = soot surface per unit volume.

2.4 Histopathology of particulate emissions

The interest in controlling soot emissions is due to the understanding that soot particles can adsorb harmful PAH onto their surfaces. Small soot particulate emissions contribute to the development of health problems; pollution of air, water, and soil; soiling of buildings; reductions in visibility; impact agriculture productivity and global climate change. Many toxicological and epidemiological studies established that exposure to combustion particulates have been linked to acute short term problems such as irritation of the eyes, nose, and throat, vomiting, light-headedness, headache, heartburn, numbness, bronchitis, chronic respiratory, cardiovascular, cardiopulmonary, allergic diseases (shortness of breath and painful breathing), cancer, and premature death (Bogarra *et al.*, 2016). Other studies have also shown that particulates can lead to inheritable mutations (Huang *et al.*, 2016).

Potential health impacts of particulate matter, ozone and carbon monoxide formed from emissions of tyre and diesel on newborn children include birth defects, growth retardation and sudden infant death syndrome. Tyre, forest fires and diesel combustion contains a variety of confirmed carcinogenic compounds such as formaldehyde, acetaldehyde, dioxins and PAHs and even oxygenated-PAHs (García-Pérez *et al.*, 2016). At least 30 toxicological studies link diesel exhaust to lung cancers (Akbaba and Kurt, 2016). Other Studies have linked tyre soot to bladder cancer (Robjohns *et al.*, 2015). On average, long-term occupational exposures to particulates have been associated with an increase of ~ 40% in the relative risk of lung cancer (Tomczak *et al.*, 2016). A case study based on population identified statistically significant increases in lung cancer risk for truck drivers, rail, road workers and heavy equipment operators especially in the thermal degradation of tyre.

Several organizations have reviewed epidemiologic and pathological experimental studies related to aerosols and lung cancer (Pease *et al.*, 2016). They have proposed classifying particulates especially those from exhaust emissions as “potential, likely, probable, or definite’’ carcinogens for humans (IARC, 2005; White, 2008). Apart from the health

problems soot combines with other air pollutants to form atmospheric brown clouds (ABCs) which cause numerous adverse environmental health effects (Thurston *et al.*, 2016).

Extensive studies analyzing the effect of diesel emissions exposure in rats have demonstrated increased accumulation of particles and aggregates of particle laden macrophages in the alveoli and per bronchial interstitial tissues as well as local inflammation, epithelial proliferation, fibrosis and emphysematous lesions (Noël *et al.*, 2016). Diesel emissions are associated with reproductive system impacts in animals. Pregnant rats exposed to diesel emissions exhibited elevated testosterone in the mother and reproductive organ changes such as masculinization of fetuses. Animal studies suggest soot particulate emissions may affect the immune system, eventually leading to a compromised immunity to bacterial infections in the lung (Pardo *et al.*, 2015).

2.5 The toxicological impacts of soot

Soot particulate has now become an issue in the global environment due to the health problems and environmental degradation it causes. Animal studies on rats exposed to soot nanoparticles of 22 nm diameter has shown that soot particulates can be translocated to the connective tissue of the heart (fibroblasts) (Geiser *et al.*, 2005). Within 30 minutes post exposure, large quantities of intra-tracheally instilled soot nanoparticles (30 nm) have been found in platelets in the pulmonary capillaries of rats (Oberdörster *et al.*, 2005).

Soot particulates are known to increase morbidity and mortality rates. Soot toxicity is a subject of both environmental and biological concern. Vehicular exhaust from combustion of gasoline, diesel, and other petroleum fuels is a dominant contributor to fine ($PM_{2.5}$) and ultrafine ($PM_{0.1}$) particulates and contains emissions of carbonaceous particles with fused and free polycyclic aromatic hydrocarbons (PAHs) (Pey *et al.*, 2009). PAH metabolism through phase xenobiotic metabolism generates electrophilic and reactive metabolites that have been indicated as inducers of pulmonary cytochrome P450 in diesel exhausts particles (Rengasamy *et al.*, 2003). Furthermore, ambient PM contains persistent free radicals and reactive oxygen species (ROS) implicated in the generation of cellular oxidative stress (Dellinger, WA.Pryor, *et al.*, 2001; Baulig *et al.*, 2003).

Depending upon the chemical characteristics of burning materials and environmental conditions, such as temperature and oxygen content, the amounts and particulate size of soot products, gases, and other volatiles generated vary from fire to fire (Chaturvedi, 2010). The ultrafine small particulates are more harmful to human health than are the large particulates.

The soot particulate matter having a diameter less than 2.5 µm are called $PM_{2.5}$ and they are capable of by-passing the body's respiratory filters and penetrating deep into the lungs (Wang *et al.*, 2013). For instance, in children fine particles of soot are associated with upper and lower respiratory impact, as well as retardation of lung growth and crib death (Kenley *et al.*, 2011). Soot as a poison leads to development of respiratory diseases such as asthma, emphysema, and consequently cancer (Barfknecht, 1983; Pope *et al.*, 2002). Soot reduces pulmonary function and causes irritation of the respiratory tract. These symptoms occur at concentrations of soot above 3.5 mg/m^3, according to the Occupational Exposure Safety and Health Administration (OSHA) (Thomas *et al.*, 2000). Women exposed to high levels of PM_{10}, (especially those coated with PAHs) have been observed to give birth to children with defects. Such children are slow to learn and face an increased risk of cancer (Wang *et al.*, 2013).

2.6 Visibility

This is the distance at which an object can be just perceived against the horizon sky. The airborne particulates scatter the sunlight and reduce the light flux. As a result, the contrast between the objects and their background gets diminished and visibility becomes impaired. The fraction of light scattering by any one particle is called the *single scattering albedo*, denoted by *w0* (Cheng *et al.*, 2015). This single scattering albedo depends upon the diameter of the particulates. Those having the size ranging from 0.1 nm to 1.0 nm have a high value of *w0*, since their diameters are comparable to the wavelength of visible light. Hence, this causes a significant reduction in visibility (Dong *et al.*, 2015).

2.7 Odour

Soot particulates are involved in the transmission of unpleasant odours. Some particulates are volatile and therefore, their odours spread from one place to another. Some aerosols are non-volatile and do not possess any odour, however, they serve as a transport medium for volatile matter which possess odour (O'Dowd *et al.*, 2002). For instance, odours from incinerators, open-dump fires and food products are transmitted by particulates (Köhler and Allgeier, 2015).

2.8 Soiling and damage to materials

Soiling is an optical effect which is essentially the darkening of reflectance that results from the deposition of airborne particulate matter to exterior building or structure surfaces. Therefore, an important part of soot particle pollution is the soiling of man-made surfaces.

Hence, the processes of cleaning, painting and repairing exposed surfaces become an economic burden. Chemical degradation of materials due to deposition of atmospheric acid particles (especially sulphur from tyre burning) is an important aspect of material damage (Guidotti, 2016). Since airborne particulate matter is of two classes, PM_{10} and $PM_{2.5}$, they differ not only in size but also in source, chemical composition, physical properties and their formation processes. In addition, the soot damages painted surfaces such as walls, doors and automobiles. Soot deposited on urban buildings imparts an unaesthetic appearance. The deposition of soot on fabrics also lowers their texture and lifespan (Dong *et al.*, 2015).

The degree of soiling is influenced by the optical and chemical compositions of airborne particulate matter. Saffaripour *et al.* (2015), observed that a diesel soot particles are about 3.5 times blacker than the average urban particulate. Hence, diesel smoke tends to stick to surfaces more than average particulates. The authors compared the reflectance of diesel soot with known reflectance of average urban particulates. They concluded that only 1/3 to 1/4 of the mass of diesel soot compared with urban particulates was required to achieve a stain of equivalent darkness. Hence, diesel soot is expected to have a greater affinity to surfaces than generated atmospheric particulates. The liquid components of diesel particulates allow it to adhere to a surface more readily than dry average particulates (Maricq, 2007). Diesel soot has a greater tendency to smear and is more difficult to remove than dry particulates due to its liquid components (Andrews *et al.*, 2013).

2.9 Significance of this study

This study characterized and identified the toxic compounds formed from selected combustion sources i.e. tyre burning, forest fire and motor exhaust. The energetics of selected PAHs/long chain hydrocarbons and their corresponding free radicals were explored using high level quantum mechanical calculations of Density Functional Theory (DFT/B3LYP) in conjunction with 6-31G basis set. The surface morphology and particle size distribution of soot was characterized by scanning electron microscopy (SEM) in conjunction with Igor and Image *J* computational softwares. Moreover, this study identified new organic compounds in combustion sources especially forest fire, building upon the qualitative analysis of previous study. Particular emphasis was placed upon characterizing unique organic compounds that may serve as tracers for this source to identify and quantify their presence in future atmospheric studies. The study also provides the first side-by-side comparison of emissions from the open combustion of forests, tyres and diesel *in situ* and in the laboratory. With

parallel methods of sample collection and analysis, we can understand the differences in combustion of various combustion sources and laboratory measurements, including the effects of dilution of emissions and chemical aging. These comparisons provide information as to what effect these parameters have on combustion emissions. Finally, the understanding of the composition and quantity of organic compounds emitted from these three combustion sources is important to evaluating the extent of human population exposure by investigating behavioural nature of the mice and qualitative bio-assay of tissues exposed and non-exposed tissues to various types of soot for their toxicological impacts on mice.

CHAPTER THREE

MATERIALS AND METHODS

3.1 Materials

The reagents used in this study were of analytical grade (purity ≥ 99%). Methanol and dichloromethane were purchased from Sigma Aldrich, Inc., St. Louis, Missouri, USA. Clean tyre samples were obtained from a tyre waste yard while diesel was purchased from a local retail outlet and used without further treatment.

3.2 The combustion reactor system

The combustion reactor used for the simulation of forest fire was fabricated by a local *Jua Kali* artisan and comprises of three major parts i.e. the feedstock cage, chimney and the funnel as shown in Figure 3.1. The funnel traps the gas-phase particulate emissions and directs it to the chimney. The chimney is connected to a porous tube that directs gas phase emissions to a solvent in a conical flask. This is a self-developed porous tube which prevents the loss of fine particles and semi-volatile vapours when sampling is carried out from high temperatures and open burning. This allows reliable sampling from harsh conditions, such as in-furnace sampling of aerosols. The dimensions of the reactor were 28 × 24 × 20 cm.

Figure 3.1: Reactor assembly for the simulation of a forest fire

For the case of tyre, the reactor used was a muffle furnace (Thermo-Scientific), USA whose internal heating compartment has dimensions of 5 cm × 6 cm × 8 cm. The heater is fitted with a temperature regulating knob. The temperature of the heater ranges from 20 °C to 1000 °C. At the top of the heating compartment is a hole which allows the gas-phase trapping tube to pass through. The sample holder in the heating compartment was quartz reactor of dimensions: i.d. 1 cm × 2 cm (volume ≈ 1.6 cm^3) fitted with gas collecting tube which can withstand high temperatures of up to 1200 ˚C. The reactor system used in this study is presented in Figure 3.2 below

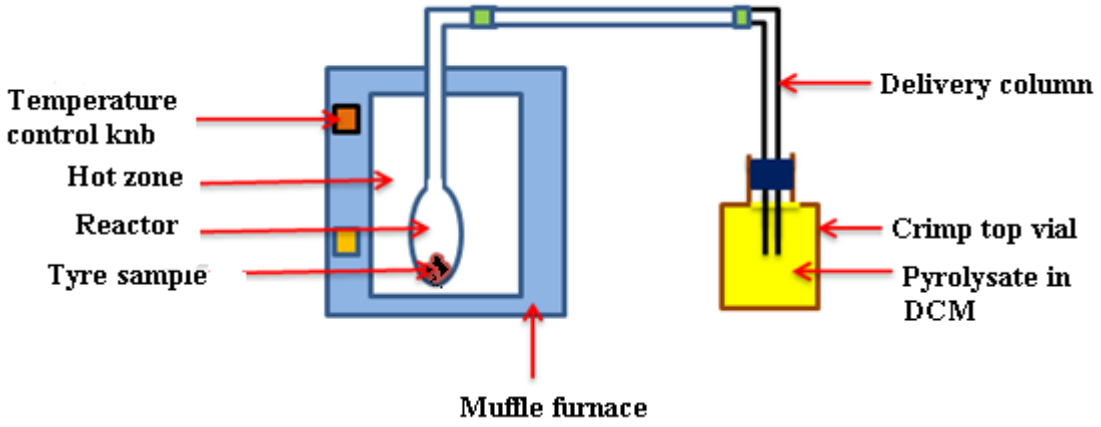

Figure 3.2: Reactor assembly and the tyre gas-phase trapping apparatus

3.3 Collection of soot from forest fire simulation

The feedstock for forest fire included different species of plants i.e. woodchips from forest residues and fresh plant materials of nineteen different plant species were collected, mixed and used as raw material for simulated forest fire. The nineteen plant species were: *Eucalyptus globus, Acacia abyssinica, Fam mimosaceae, Spathodea campanulata, Prunus africana, Dombeya torrida, Todalia asitica, Croton megalocarpus, Hagenia abyssinica, Albizia gummifera, Albizia lebbeck, Markhamia lutea, Erythrina abyssinica, Cynodon nlemfuensis, Digitaria scalarum, Tagetes minula, Biddens pilosa, Croton elliotanus and Cupressus bakerii*. These materials were obtained from Egerton University botanical garden (Kenya). The plant species were identified and then arranged in the reactor for forest fire simulation and soot collection whereby its gas phase was dissolved directly into dichloromethane through a porous tube diluter. The volatile extracts were then transferred into amber vials for GC-MS analysis. The char was also packed in amber vials for SEM analysis.

3.4 Particulate emissions from the thermal degradation of waste tyre

Tyre is composed of different components (rubber, carbon black, steel, fillers, and sulphur as the major components), which additionally are heterogeneously distributed along the tyre. Therefore in order to investigate a representative sample of the whole tyre, a cross-section piece of 4–6 cm wide and 8-9 cm long (≈200 g) of a commercial car tyre was used in the pyrolysis experiments. The larger piece was sliced into small pieces in order to fit in the reactor. Tyre burning was conducted in a quartz reactor of dimensions ~ 1.6 cm^3 as described in section 3.2. The gas phase components were passed over dichloromethane (DCM) and packaged into 2 mL vials for analysis using a GC-MS. The soot/char was also packaged in amber vials for SEM analysis.

For determination of percentage yield of tyre sample in terms of volatiles emitted, another tyre sample was heated at various temperatures; 200, 250, 300, 350, 400, 450, 500 and 500 °C at a constant residence time of 10 minutes. The residue formed at every pyrolysis temperature was collected and weighed in order to determine char yields.

3.5 Soot collection from vehicular exhaust

The gas phase of the exhaust soot was trapped directly from the motor exhaust diesel vehicle (lorry) and immediately dissolved in dichloromethane through a partial exhaust flow dilution system (porous tube diluter). The dissolved sample was then stored at room temperature (25 ^{o}C) for analysis using GC-MS.

3.6 Gas Chromatography-Mass Spectrometer (GC-MS) Analysis

Organic by-products from tyre and diesel burning was passed through 10 mL dichloromethane solution (DCM), filtered using a filter paper (Whatmann no. 10) and investigated using Agilent 6890 Gas chromatograph hyphenated to an Agilent mass selective detector (MSD), 5890 series. About 1 µL of filtered sample was injected into a GC column (DB-5MS, 30 m × 250 um × 0.5 µm). The temperature of the injector port was set at set at 200 °C to enable the conversion of organic components to the gas-phase prior to MS analysis. Temperature programming was applied at a heating rate of 15 °C for 10 minutes, holding for 1 minute at 200 °C, followed by a heating rate of 25 °C for 4 minutes, and holding for 10 minutes at 300 °C. Electron Impact ionization energy of 70 eV was used. Molecular products were identified using the National Institute of Science and Technology software (NIST, USA) and confirmed by enhanced data incorporated into the Chemstation of Agilent's MSD

(Kibet *et al.*, 2012). To ensure the correct compounds were reported, the peak shapes and the retention times of molecular products with those of pure compounds (standards) were compared, and found to match with remarkable accuracy.

3.7 Scanning Electron Microscopy (SEM) analysis

Soot samples were heated from ambient temperature to 600 ^{o}C at a heating rate of 5 $^{\circ}$C min^{-1} under an inert N_2 gas flow. A gold coating of 9 nm (prepared using 6nm by 1.5 nm layers) was applied to the stub to reduce charging of the non-electrically conductive particles. A JEOL JMS 7100F SEM was used to image the soot. To aid identification of the soot, elemental analysis of both Pt and F was conducted using Noran system seven version 3.1 Ultra dry SSD X-ray detectors (EDX). For improved image clarity, a second sample of soot was coated with a 3 nm Au layer to allow higher resolution images to be obtained. All images were captured at an angle of 45^{o} to improve definition of surface morphology.

3.8 Computational methodology

In order to investigate the molecular behavior and energetics of volatiles which was identified in this work, thermochemical calculations were conducted using Gaussian '09 computational platform (Frisch *et al.*, 2009). The geometries were optimized at DFT/B3LYP using the 6-31G basis set (Zhang *et al.*, 2010). Diffuse and polarization functions included large atoms because they were necessary in the optimization of large molecules and radicals, that is, polarization functions were also added on hydrogen atoms in order to account for the presence of hydrogen-bonds (Saron *et al.*, 2008). Chemissian *ver.4.38* computational software was used to model molecular orbital energy level diagrams, electron density maps as well as determine the band gap energies of frontier orbitals (HOMO-LUMO) (Lenoid, 2012) for the selected organic volatiles (PAHs).

3.9 Experiments involving research mice

3.9.1 Mice handling

Eleven male mice (*M. musculus*) of eight to ten weeks old were purchased from Kenya Medical Research Institute (KEMRI). All mice were housed at the Biological department together with the inhalation facility within Egerton University, in a 20 × 43 × 18 cm polycarbonate cages with a wire-top system containing Tech pellet/corn-cob bedding in temperature and humidity controlled rooms. The mice were divided into four groups, that is, three for vehicular exhaust soot, three for tyre soot, three for simulated forest fire soot and

two control mice. They were maintained on a 12-hour-light/12-hour-dark cycle. The mice were provided with standard chow and they were allowed to acclimate for one week prior to the experiments. All animal procedures and handling was performed in accordance with standards established by the Kenya Animal Welfare Acts as set by the National Guidelines for the Care and Use of Animals in Research and Education in Kenya (Kimwele *et al.*, 2011).

3.9.2 Soot particulate exposure protocol for albino mice

The aim of this study was to define the effects on the lung tissues of mice resulting from whole-body exposure to soot. During exposure periods the wire-top lid was replaced with a sealed top and high-efficiency airflow system to deliver gaseous particulate by unidirectional flow. Mice were exposed to soot from the different sources by whole-body exposure for 6 hours (two hours in the morning, two hours in the afternoon and two hours in the late evening respectively) per day for 14 consecutive days. During exposures, animals were provided with food pellets but no water to reduce wet conditions and therefore prevent dilution effect. Pulmonary response to exposure was evaluated after each soot exposure protocol is completed.

Within 2 hours of completing the 14-day exposure protocol, mice were sacrificed by euthanizing with sodium pentobarbital/chloroform first, then dissecting them to remove and analyze the organs of interest (Yu *et al.*, 2002). The trachea was exposed, cannulated, and secured with a suture. The lungs were immediately removed from the thorax and frozen in liquid nitrogen. Twenty-four hours later, a portion of the lung tissue was homogenized in 0 ^{o}C Tris-hydro-chloride (CH_2C (CH_2OH) $_3$.HCl) buffers (25 mM Tris, 1 mM EDTA). The lungs were lavaged four times with a single volume of phosphate-buffered saline. Then the samples were analyzed for damage or any change caused by soot. Thereafter, the test organs and other carcasses for the experimental mice were incinerated in the Animal Health department incinerator of Egerton University.

3.9.3 Mice respiratory tissue analysis

Qualitative bio-assay of tissues exposed and non-exposed to various types of soot was investigated for their toxicological impacts on model mice. The behavioral nature of the mice was monitored over time after exposure to exhaust soot, forest fire soot, and soot from tyre combustion at an interval of six hours. The mice were then dissected for internal damage examination caused by soot inhalation. To determine biological effect of soot exposure,

texture, colour and shape of lung tissues of health mice (control) were compared with those of mice exposed to soot. Here, micrographs were taken using a Light Microscope interfaced with a computer for comparison.

3.10 Data analysis and presentation

Igor and Image *J* computational softwares were used to analyze images. One-way analysis of variance (ANOVA) was performed to compare the concentration of toxic compounds formed during combustion. A t-test was used to compare mean sizes of soot particles formed. Data was presented in form of micrographs, images and tables.

CHAPTER FOUR

RESULTS AND DISCUSSION

4.1 Molecular distribution of organic volatiles from selected combustion sources

In these experiments, critical molecular components of soot particles were detected. This includes; long chain hydrocarbons, large cyclic hydrocarbons, PAHs and oxygenated hydrocarbons. These results are remarkable. They suggest that there must be a clear distinction between soot particles and the volatile components of combustion. Therefore, our experiments have demonstrated that soot 'black carbon' could be a rigid mass of PAHs which could not be dissolved by organic solvents to allow for detection. The following sections gives some of the molecular compounds detected during the combustion of various biomass materials (simulated forest fire), combustion of diesel (vehicular soot), and tyre burning. Interestingly, all the three sources of soot investigated in this experiment gave similar molecular products although at different intensities.

4.2 Molecular volatiles from simulated forest fire

This study was able to identify various molecular organic toxins from simulated forest fire. These included aromatic hydrocarbons, oxygenated combustion by products such as dibenzo-*p*-dioxin, 2H-benzopyran, long chain oxygenated hydrocarbons, and long chain hydrocarbons. Their intensities varied significantly. For instance, the long chain oxygenated hydrocarbons and long chain hydrocarbons were abundant in particulate emissions while the aromatics were found in low concentrations.

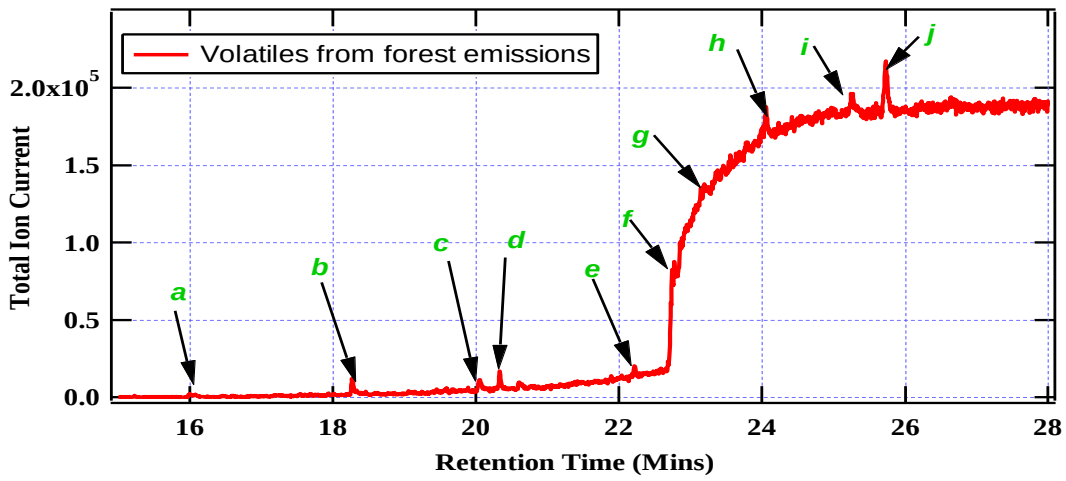

Figure 4.1: GC-MS chromatogram for selected volatiles from forest fire

The volatiles which were detected in this study under simulated forest fire were molecular compounds characterized by long chain hydrocarbons. These include tricosane, tricosene, octadecenoic acid, nonadecene. However, there was also detection of dibenzo-*p*-dioxin, 2H-benzopyran, benzene, naphthalene, and methanoic acid (Table 4.1). The GC-MS chromatogram for forest fire volatiles is reported in Fig. 4.1, *vide supra*.

Table 4.1: Volatile components from simulated forest fire identified using GC-MS

No	Molecular toxin	Molecular structure	Retention time (mins)	Molecular mass (g/mol)
A	Benzene	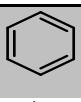	16.12	78.05
B	Indene	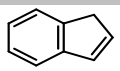	18.38	116.08
C	Methoxy acetic acid	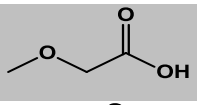	20.15	90.03
D	2H-benzopyran	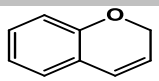	20.37	132.06
E	Cyclopropaneoctanal		20.53	168.15
F	Dibenzo-*p*-dioxin	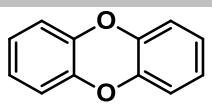	22.40	184.19
G	Phthalic acid	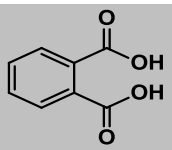	22.83	166.03
h	Oleic acid		24.15	282.26
I	Tetracosane		25.35	338.39
J	Cyclotetracosane	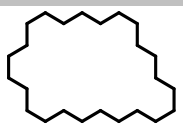	25.79	336.38

These compounds are discussed further because of their characteristic behavior to cause serious environmental and biological concerns. At reasonably high temperatures, these compounds may transform to more dangerous products and cause serious ailments to biological systems as discussed in section 4.5. Table 4.1 presents the molecular structures of major GC-MS compounds detected in this study. For instance, dibenzo-*p*-dioxin which has the ability to convert into the poisonous chlorinated dibenzo-*p*-dioxins under conditions desirable reported elsewhere (Evans and Dellinger, 2003, 2005; Kibet *et al.*, 2013).

The abnormal rise in the baseline for GC-MS analysis can be attributed to the dirty nature of samples from forest fire as the temperature increases. Increase in temperature is usually accompanied by high pressure and thus the rise in the GC-MS baseline. Although the molecular products detected using GC-MS were of low intensities (Table 1), these compounds are considered toxic. For instance benzene and naphthalene are well-established carcinogens (Junjie *et al.*, 2014). They can metabolize in the body system to yield more toxic components such as quinones (Bolton *et al.*, 2000). The toxicology of these compounds will be discussed subsequently in brief (section 4.3).

4.3 Molecular toxins emission from tyre and diesel

Most molecular toxins from fuel combustion are mainly hydrocarbons, especially PAHs. The GC-MS chromatograms for molecular volatiles from tyre and diesel burning are presented in Figures 4.2 and 4.3 respectively. Polycyclic aromatic hydrocarbons are organic compounds that consist of two or more fused aromatic rings and are known to have mutagenic and carcinogenic effects. Their main source is the incomplete combustion of carbon-containing materials including coal, biomass and gasoline and diesel fuels. Their structures lead to many different ring arrangements, which give rise to a wide range of isomers. Thirteen major compounds of molecular mass ranging from 78.05 (benzene) to 254.33 g/mol (benzo[a]pyrene) were identified from the combustion of diesel sample (Table 4.2). The GC-MS chromatograms for the organic volatiles (PAHs) identified from combustion of diesel are indicated below.

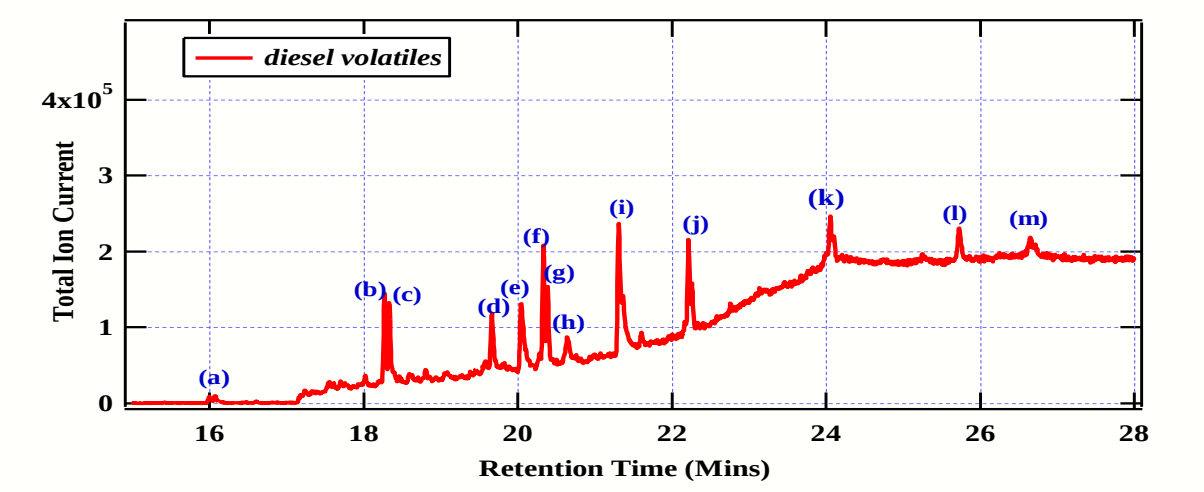

Figure 4.2: GC-MS chromatogram for selected volatiles from diesel combustion

From the above GC-MS chromatograms the following tabulated compounds were elucidated with help of the NIST library.

Table 4.2: Organic volatiles from the thermal degradation of diesel sample

No	Molecular toxin	Molecular structure	Retention (mins)	Molecular mass (g/mol)	formula
A	Benzene	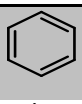	16.12	78.05	
B	Indene	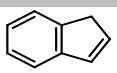	18.38	116.08	
C	Benzaldehyde	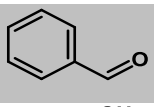	18.41	106.04	
D	*o*-cresol	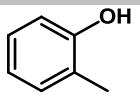	19.85	108.14	
E	Benzofuran	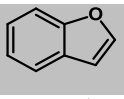	20.15	118.13	
F	Fluorene	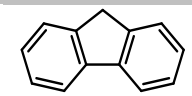	20.43	166.22	
G	Anthracene	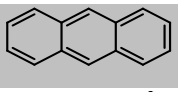	20.51	178.08	
H	Phenanthrene	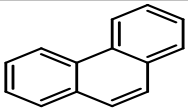	20.78	178.08	

I	Fluoranthene	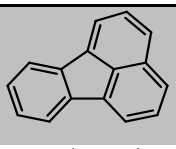	21.62	202.08
J	Pyrene	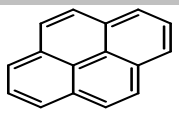	22.40	202.08
k	Chrysene	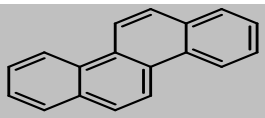	25.84	228.09
L	benzo[a]pyrene	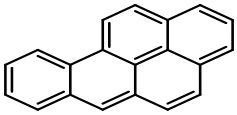	26.89	252.09
m	2-phenylphenanthrene	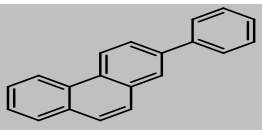	24.22	254.33

The above results show the dominance of some compounds over others. For instance, the GC-MS chromatograms above (Fig. 4.2) show the four PAHs with the highest concentrations as observed during the thermal degradation of diesel i.e. the indene (two ringed), fluorene (three ringed), fluoranthene (four ringed) and pyrene (four ringed). Indene is the lightest of the four PAHs with a molecular weight of 116.08 g/mol while the other three most abundant PAH have a molecular weight of 166.22 for fluorene and 202.08 g/mol for pyrene and fluoranthene respectively.

The enhanced concentrations of PAHs are largely in the higher molecular weight range. This study reveals that four or less membered ring PAHs are in gaseous phase which is in agreement with previous studies that two to four ring PAH are primarily found in the gaseous phase, while five to seven ring PAH are primarily found in the particulate phase. Whereas thirteen volatile compounds (PAHs) were identified from diesel combustion, eight major PAHs were identified from the thermal decomposition of tyre (Figure 4.3).

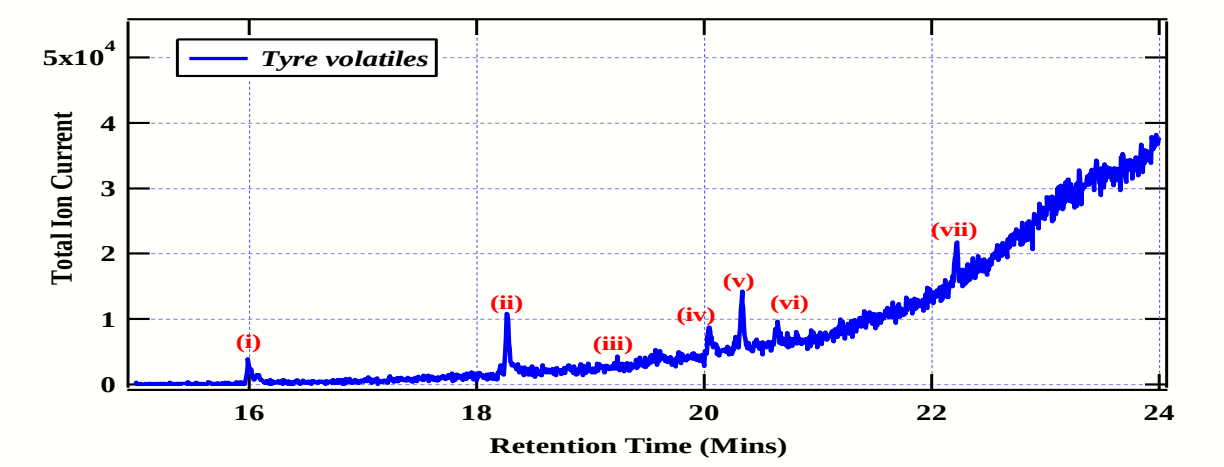

Figure 4.3: GC-MS chromatogram for selected volatiles from tyre combustion

With the help of NIST library and Chemstation the following compounds for the tyre combustion;

Table 4.3: Organic volatiles from the thermal degradation of tyre

No	Molecular toxin	Molecular structure	Retention (mins)	Molecular formula mass (g/mol)
I	Benzene	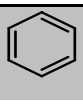	16.12	78.05
ii	Benzaldehyde	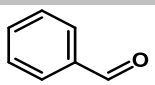	18.41	106.04
iii	Propylcyclohexane	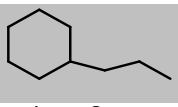	19.35	126.14
iv	Benzofuran	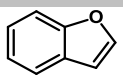	20.15	118.13
V	Fluorene	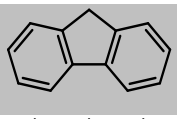	20.43	166.22
vi	Anthracene	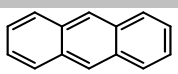	20.51	178.08
vii	Pyrene	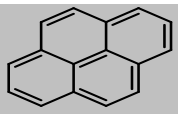	22.40	202.08

Tyre combustion also revealed varying concentrations of the various compounds, for example, benzaldehyde, fluorene and pyrene had the highest concentrations. These results imply that tyre combustion mainly generates PAHs as the major organic volatiles. Of the

eight detected compounds in this work, only three volatiles cannot be classified as PAHs i.e. benzene, benzaldehyde and propylcyclohexane. It is evident therefore from this study that diesel and tyre combustion by-products were mainly PAHs, some of which have been implicated as a series of biological ailments. The PAHs from the thermal degradation of diesel (Table 4.2) were significantly more than the PAHs derived from the thermal decomposition of tyre (Table 4.3). Nonetheless, the relative intensity of particulate emissions from tyre was significantly low. Nonetheless, tyre burning generates a lot of soot in comparison to diesel burning.

The detection of cyclopentafused PAHs mainly in the combustion of diesel (fluorene and fluoranthene) is an indication that diesel particulate emissions are very toxic. This is because cyclopentafused PAHs are more bio-active than their analogous PAHs without the cyclopenta moiety (Labota *et al.*, 2005). Fluorene was also detected in tyre burning. A few oxygenated compounds also considered xenobiotic (chemical compound that is foreign to biological systems) and eco-toxicants because of their bio-activity were detected in this investigation. This included *o*-cresol, benzaldehyde, and benzofuran. Whereas the intensities of organic toxins were very high in diesel emissions, the intensity of the same organic toxins were very low in tyre burning. However, it was noted that numerous straight chain alkanes such as tetracosane, pentacosane, decaline, nonane, and decane (although of very low intensity) were detected in our experiments. Straight chain alkanes are also well known components of particulate emissions and are conventionally established organic toxicants.

PAHs have previously been identified in tyre combustion and given the negative health impacts associated with them; their concentrations are of considerable interest. However, not all PAHs are of the same toxicity. The structure of a particle and the substituted groups determine harmful properties of PAHs. Many PAHs belong to the group of carcinogens, in particular the unsubstituted PAHs as well as the nitrated and methylated ones, and those containing the carboxylic group. Nonetheless, a significant amount of sulphur dioxide may have been evolved during the thermal degradation of tyre and this may contribute to some pathological problems observed in the lung tissues of albino mice. This is because conventionally sulphur is a major component in tyre manufacture.

4.4 Oxygenated organic volatiles

Combustion of forest biomass, tyres and diesel generates analogs of cyclic and polycyclic aromatic hydrocarbons that contain heteroatoms (May *et al.*, 2012). An oxygenated PAH

(oxy-PAH) is a PAH with one or more carbonyl functional groups. Examples of oxy-PAH structures detected in this work are shown below.

Figure 4.4: Oxygenated volatiles detected in this study

Oxy-PAHs have been measured in the environment and are detected in particulate matter emitted by combustion sources such as waste incineration, petrol and diesel emissions, bio-mass burning and tyre combustion which are inclusive in this study. Oxy-PAHs have also been shown to undergo some reactions (secondary reactions) as a result of parental PAHs combining with atmospheric oxidants like hydroxyl radicals. The presence of heteroatoms in these polycyclic compounds changes their interactions with biological tissues, giving them different health effects, when compared to PAH. Carbonyl functional groups on PAH do not increase mutagenic properties of these compounds however their oxyl radical are very can cause serious cellular damage.

4.5 Molecular toxins that may easily transform into hazardous products

Although it would appear that a few volatiles are detected in this study, many minor molecular compounds characterized by long chain hydrocarbons were also detected. These include tricosane, tricosene, octadecenoic acid, nonadecene. Interesting molecular compounds of environmental concern were also identified; 2H-benzopyran and 1, 2-benzene dicarboxylic acid. These two compounds will be discussed further because of their characteristic behavior to cause serious environmental and biological concerns. At reasonably high temperatures and in presence of small amounts of chlorine and a transition metal such as iron or copper, they can convert into the most toxic class of compounds referred to as benzofurans usually implicated in various poisoning episodes of humans and animals (Evans and Dellinger, 2003, 2005; Kibet *et al.*, 2012; Nganai *et al.*, 2012), and are by far the most dangerous organic toxins to be identified in the environment in recent times. Fig. **4.5**, below,

presents the molecular structures of 2H-benzopyran and 1,2-benzene dicarboxylic acid which have the ability to convert into benzofurans under conditions desirable for the formation of such compounds (Kibet *et al.*, 2013).

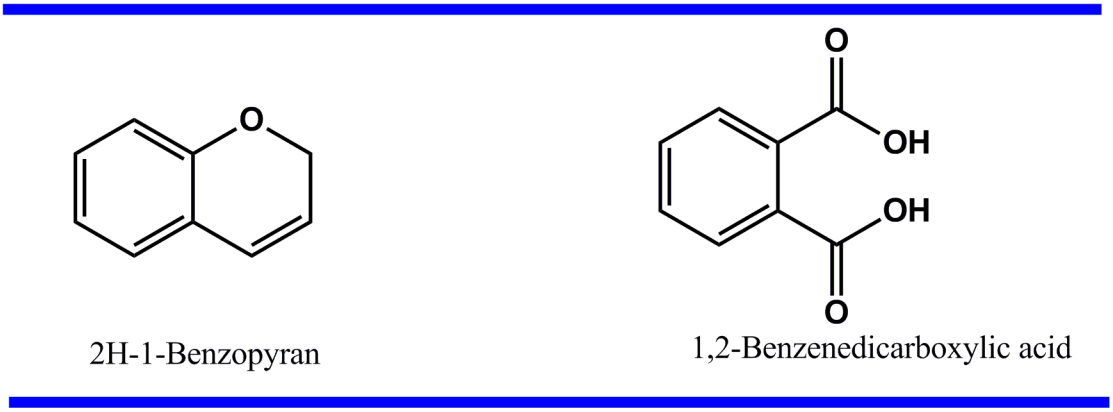

Figure 4.5: Benzofuran like structures of some molecular compounds identified in this work

4.6 Decomposition profile of waste tyre

The lowest mass loss from tyre combustion was recorded at a temperature of 200 °C and 550 °C. This means that the temperature of 200 °C is not sufficient to effect evolution of organic volatiles. Again at 500 °C most volatiles had been emitted at temperatures between 250 °C and 500 °C. These mass loss effects are well shown in the curve below (Figure4.6). Initially, there was a slight decrease in percentage char yield at 200 °C and 250 °C. However, between 300 °C and 500 °C there was drastic change in % yield.

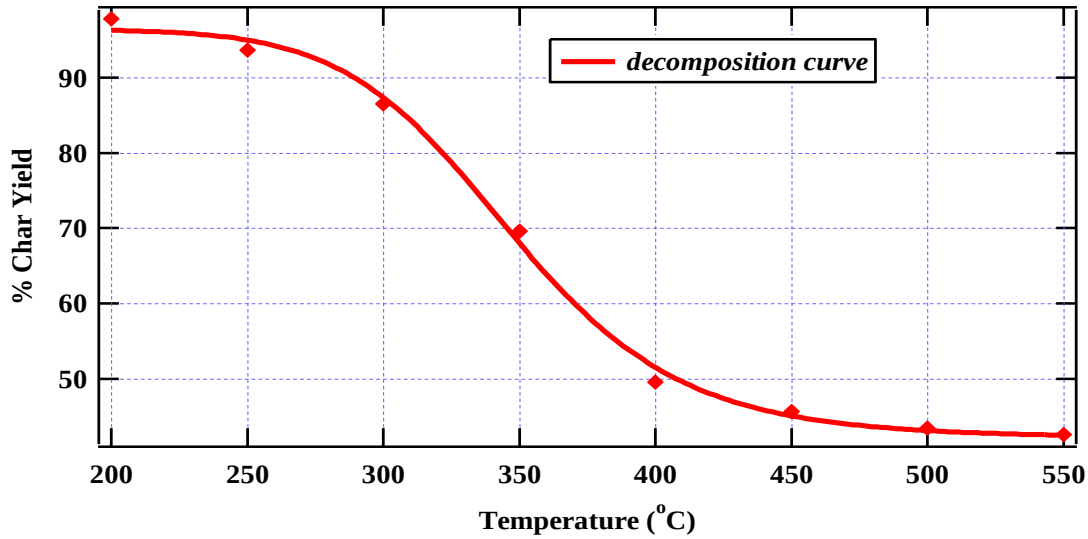

Figure 4.6: Char percentage (%) yield from thermal degradation of tyre

The decrease may be associated with high mass loss due to emission of moisture and volatiles especially PAHs such as fluorene and fluoranthene. This observation is in agreement with other results of biomass and tyre combustion which indicate that high mass loss occurs between 400 °C and 500 °C (Sharma and Hajaligol, 2003). The mass loss between 450 °C and 500 °C was ~39.2%. This region corresponds with the highest release of molecular organics. Thus, by 500 ˚C most organic compounds will have been formed so that any further increase in temperature results in sharp decrease in the thermal degradation products (Fig. 4.6). These results corroborate previous data reported in literature on thermal degradation of tyre (Kibet *et al.*, 2015; Ding *et al.*, 2015).

4.7 Characterization of soot organic volatiles from fuel combustion

At an associated magnification of ×400, the particulate soot of tyre and simulated forest fire soot were examined. The micrographs of forest fire soot were remarkably interesting. It was arduous to get a clear image of the soot in the whole range of magnification. However, we managed to obtain a somewhat neat image after several trials as shown below.

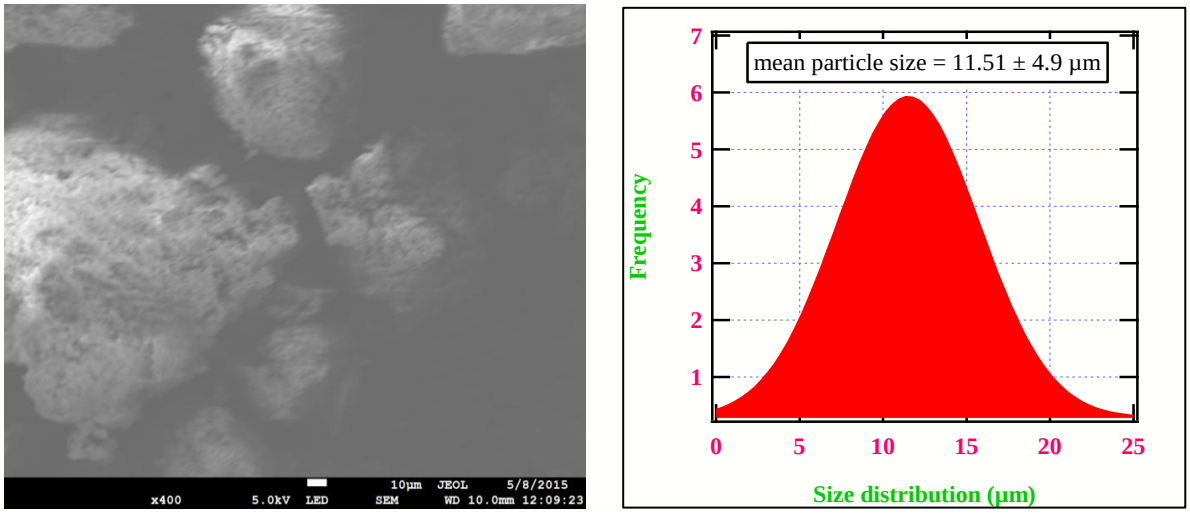

Figure 4.7: SEM image and particle size distribution (Gaussian red) of soot particles from simulated forest fire

Image J was used to measure the sizes of the soot and size distribution was predicted using *Igor* software. The mean diameter of the soot was found to be 11.51 ± 4.9 µm (cf. Fig. 4.7). This size of 11.51 microns is ~10 micrometers, hence can be classified as PM_{10}. PM_{10} is among the most harmful air pollutants. When inhaled, they evade the respiratory system's natural defenses and lodge deep in the lungs. Health problems begin as the body reacts to these foreign particles. PM_{10} can increase the number and severity of asthma attacks, cause or aggravate bronchitis and other lung diseases, and reduce the body's ability to fight infections.

Though particulate matter can cause health problems to almost everybody, some people are more vulnerable to PM_{10} adverse health effects. These "sensitive populations" include children, the elderly, exercising adults, and those suffering from asthma or bronchitis. These adverse health effects are greatly dependent on the deposition and retention times of these particles in the body. This means that the deposition probability and site of particles is governed by their aerodynamic properties, for instance size, density and shape, and the physicochemical properties like hygroscopicity (Kreyling *et al.*, 2007; Hudda and Fruin, 2016). Experimental studies have identified a range of physicochemical properties that influence the toxic and inflammatory potential of PM, and possibly particle-induced health effects. The major concerns are recent studies that link PM_{10} exposure to the premature deaths of people suffering from heart and lung diseases, especially the elderly. The particulate size of soot from tyre burning was quite large (16.23 ± 3.36 µm) (Figure 4.8). Notably, to obtain enough data points to plot size distribution curves several micrographs taken at the same magnification were used.

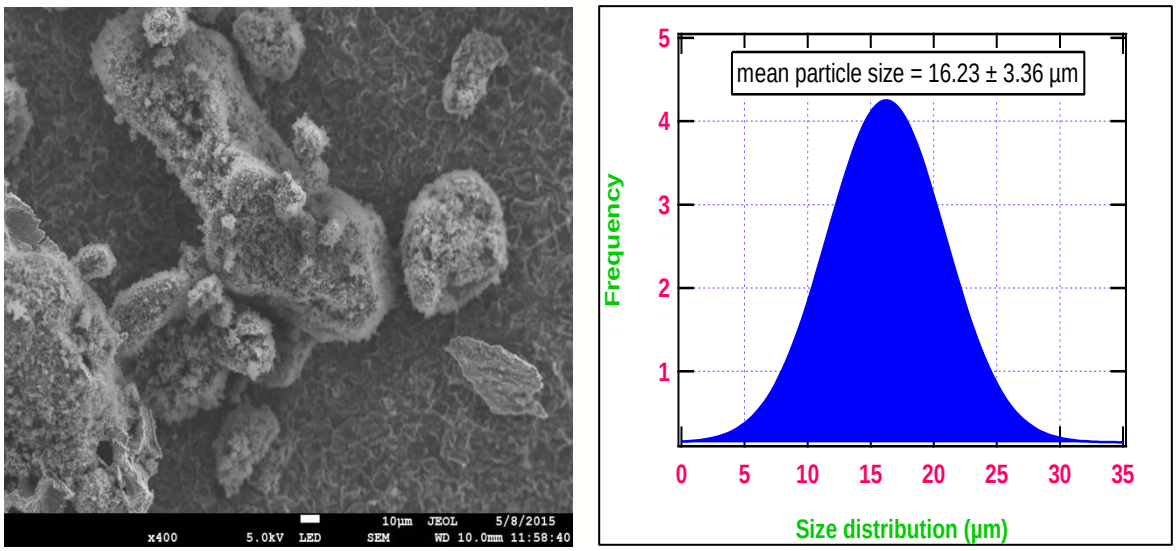

Figure 4.8: SEM image and particle size distribution (Gaussian blue) of soot particles from tyre burning

From the micrographs reported in this study, simulated forest fire particulates emissions appear smaller than those from tyre burning. Nonetheless, the two types of emissions fall within the PM_{10} category of airborne particulates. Although, these particulates are fairly, large and may not be inhaled deeper into the respiratory system, their deposition on the respiratory surface for instance the lung tissues (microphages and alveoli) may inflict serious biological damage.

4.8 Statistical analysis of particulates

Statistical analysis shown in table 4.4 based on the particulate means indicates that there is a significant difference between particulate size of tyre emissions and forest fire emissions at 95% confidence limit. The calculated F-value = 2.13 while F-critical = 1.69, confirming that the difference between the two sets of data is significant. Moreover, the P-value = 0.000 and thus less than 0.05 level of confidence.

Table 4.4: Mean sizes of particulates formed during tyre combustion and simulated forest fire

Statistical measure	**Mean**	**No. of particles**
Forest fire particulates	11.51 ± 4.90	40
Tyre particulates	16.23 ± 3.36	40

4.9 Biological health effects of molecular volatiles

Although information in literature is limited on the toxicological impacts of long chain hydrocarbons identified in this work, there is cause to conclude that they can affect respiratory organs and possibly enhance the growth of tumors along the respiratory tract. This is because these molecular compounds (α-octadecene and cyclotetracosane) are bulky and may be capable of causing health burdens when inhaled in large amounts. The fact that these compounds can possibly exhibit radical characteristics is another indication they are poisonous because radicals are reactive species which can react with biological structures inducing cell assault and consequently cell injury (Dellinger, Pryor, *et al.*, 2001; Maskos *et al.*, 2008). For instance, α-octadecene can easily exhibit radical behaviour as predicted by scheme 4.1. Whereas molecular α-octadecene may not be toxic, its corresponding free radical α-octadecenyl radical may be very toxic considering its reactive nature. Generally, at high temperatures, formation of free radicals is the predominant intermediate pathways for formation of molecular by-products. Isopulegol owing to the electron rich centre it possesses can also form a carbon centred radical in addition to the oxygen centred radical.

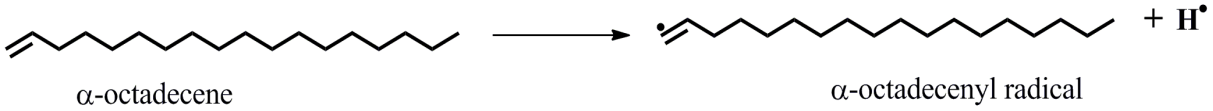

Scheme 4.1: Formation of α-octadecenyl radical (carbon-centered radical) from molecular α-octadecene

The toxicity of oxygenated molecular compounds is well documented in literature. Aldehydes for instance in this case cyclopropaneoctanal are well known toxicants classified as carcinogenic, and may be cytotoxic or genetoxic (Baker *et al.*, 2006; Lin *et al.*, 2008). Oxygenated components of combustion can form very reactive oxygen species commonly referred to as ROS. Production of ROS may result in severe oxidative stress within cells through the formation of oxidized cellular macromolecules, including lipids, proteins, and DNA (Helen and Paulson, 1997; Moridani *et al.*, 2004). This implies that methoxy acetic acid, oleic acid and isopulegol are good candidates in the production of reactive oxygen species. Nevertheless, for the purpose of this study, methoxy acetic acid and 1, 2-benzene dicarboxylic acid will be given detailed treatment to represent the characteristic behavior of other oxygenated molecular by-products of combustion in the production of reactive oxygen species (ROS).

Abstraction of an H radical by an OH radical in methoxy acetic acid results in the formation of an oxygen centered free radical as proposed in scheme 4.2. The formation of methoxy radical and the epoxide (oxiran-2-one), step 3, are proposed to proceed via the formation of an intermediate radical methoxyacetoxyl radical formed from step 2. Step 1 is proposed to proceed via the loss an OH radical from methoxy acetic acid to yield methoxyacetoxyl radical which can convert to the epoxide, oxiran-2-one, and methoxy radical via step 4. Steps 1 and 2 are competing reactions but it has been established in literature that a reaction initiated by a H radical proceeds faster than one initiated by OH radical (Kibet *et al.*, 2013). Both steps 3 and 4 form the most unstable epoxides (oxiran-2-one and oxirane respectively). Epoxides are generally quite unstable because of the strain in the molecule. Therefore epoxides are very reactive and may be the cause of various degenerative biological diseases, and environmental disasters such as explosions which may result in harmful organics.

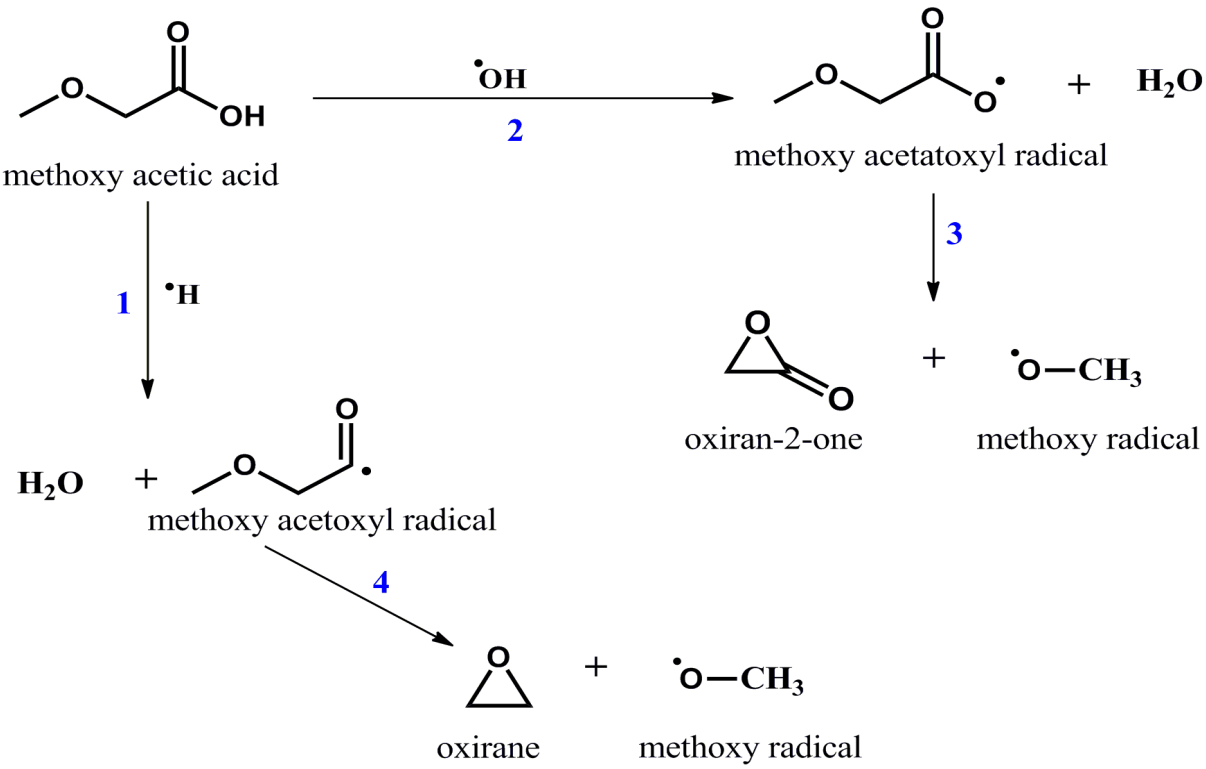

Scheme 4.2: Mechanistic formation of oxygen centered radicals from methoxy acetic acid

1, 2-benzene dicarboxylic acid can undergo dehydration reaction before ultimately forming isobenzofuran-1,3-dione or a benzoketone (bicyclo[4.1.0]hepta-1,3,5-trien-7-one) via the mechanism proposed in scheme 4.3, *vide infra*. Although short-lived, the intermediate biradical is expected to be very reactive (Dagaut *et al.*, 1996) and thus capable to damaging DNA and other cellular tissues. Hydroxyl radicals in combustion systems are a well-known candidate for initiating DNA damage and ultimately triggering the production of ROS in biological environments (Dellinger *et al.*, 2000).

4.10 Computational results

Using DFT/B3LYP computational framework in conjunction with 6-31G basis set, it was found that the formation of the biradical (scheme 4.3, *vide infra*) proceeded with a modest endothermicity of 15.21 kcal/mol. The biradical was proposed to transform into two possible products via two mechanistic pathways which were tested theoretically to determine the mechanistic channel with the lowest energy.

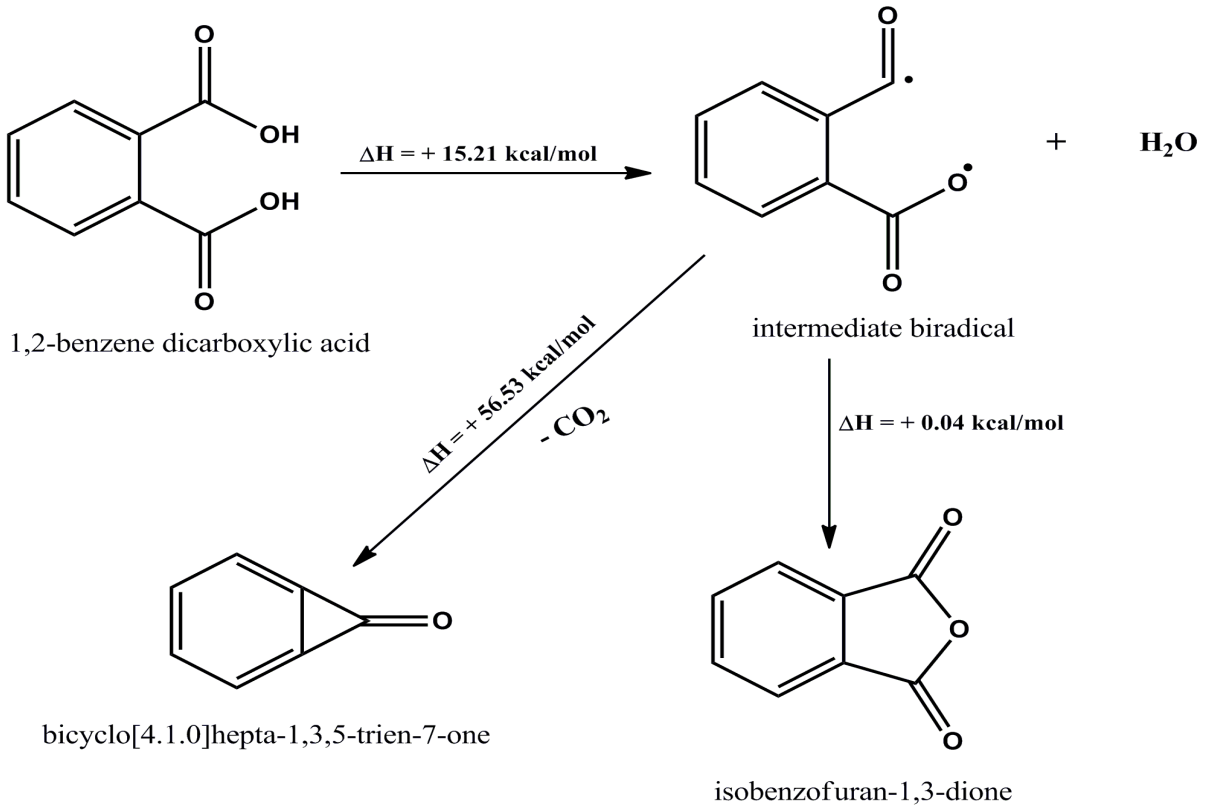

Scheme 4.3: Proposed mechanism for the conversion of molecular 1,2-benzene dicarboxylic acid to isobenzofuran-1,3-dione and bicyclo [4.1.0] hepta-1,3,5-trien-7-one.

The findings indicated that the formation of isobenzofuran-1,3-dione progressed with minimum energy of 0.04 kcal/mol and therefore highly favored compared to the decarboxylation of the biradical which proceeded with a high endothermic energy of 56.53 kcal/mol. Therefore, the decarboxylation process is not thermodynamically preferred. This explains why isobenzofuran-1,3-dione was detected in this work while bicyclo [4.1.0] hepta-1,3,5-trien-7-one was never detected or was below the detection limit of the instrument. It turns out therefore that the use of theoretical calculations is critical in predicting the possible mechanistic pathways and fate for an environmental pollutant.

Although some of the molecular volatiles discussed in this study may have no documented toxic characteristics in literature, there is a possibility they may cause cell impairment by covalently bonding with cellular nucleophiles leading to oxidative stress and other related illnesses (Sidney and Pearson, 1990).

4.11: Molecular orbitals and electron density maps

The Highest occupied molecular orbital (HOMO) and the Lowest unoccupied molecular orbital (LUMO) are conventional acronyms for the highest occupied and lowest unoccupied molecular orbitals respectively. These orbitals are the pair that lies nearest in energy of any pair of orbitals of two molecules which permits them to interact more strongly (Wyrick *et al.*, 2015). The HOMO–LUMO band-gap energies for some selected PAHs are presented in Table 4.5. The reactivity index (band gap) of the compounds with small difference implies high reactivity whereas large difference in band-gap energy implies low reactivity. Benzo[a]pyrene has the smallest HOMO–LUMO energy gap (0.072 eV) and therefore more reactive compared to fluorene (0.150 eV) and fluoranthene (0.122 eV). This implies that benzo[a]pyrene is more reactive than fluorene and fluoranthene.

Table 4.5: Band-gap energies for the PAHs investigated in this work

Compound	HOMO (eV)	LUMO (eV)	$\Delta E=E_{LUMO}-E_{HOMO}$ (eV)
Fluorene	-0.353	-0.203	0.150
Fluoranthene	-0.345	-0.223	0.122
Benzo[a]pyrene	-0.315	-0.243	0.072

The band-gap energy between the HOMO and the LUMO is directly related to the electronic stability of the chemical species. This means that benzo[a]pyrene having a lower HOMO energy value of −0.315 eV is much more stable making it a good nucleophile compared fluorene (-0.353 eV) and fluoranthene (-0.345 eV) which are energetically higher in the HOMO (Parr and Pariser, 2013). The HOMO-LUMO energies of these PAHs are low and correspond to their potential reactivity towards biological systems. The molecular orbital profile for fluorene is presented in Figure 4.9

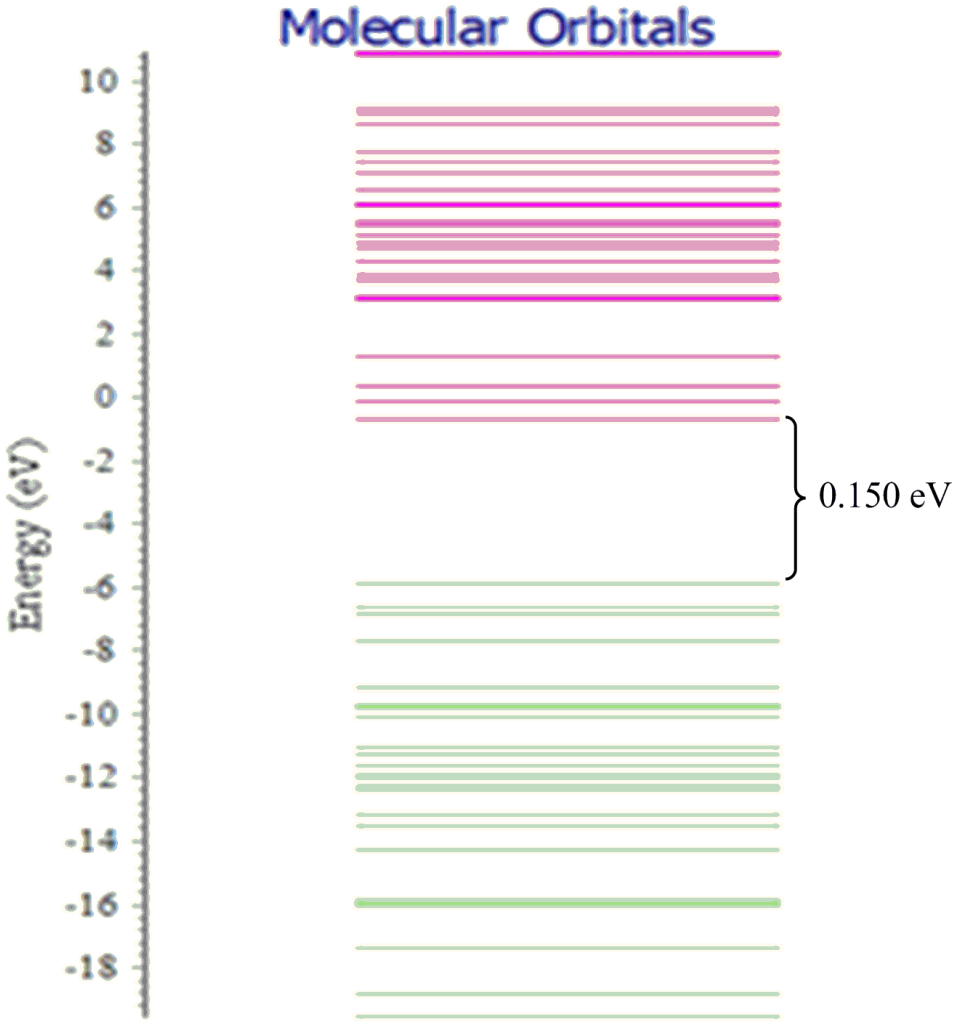

Figure 4.9: The HOMO-LUMO band gap for fluorene determined using Chemissian

The construction of 2-D and 3-D electron density contour maps for fluorene was achieved using Chemissian computational code and reported in Figures 4.10 and 4.11.

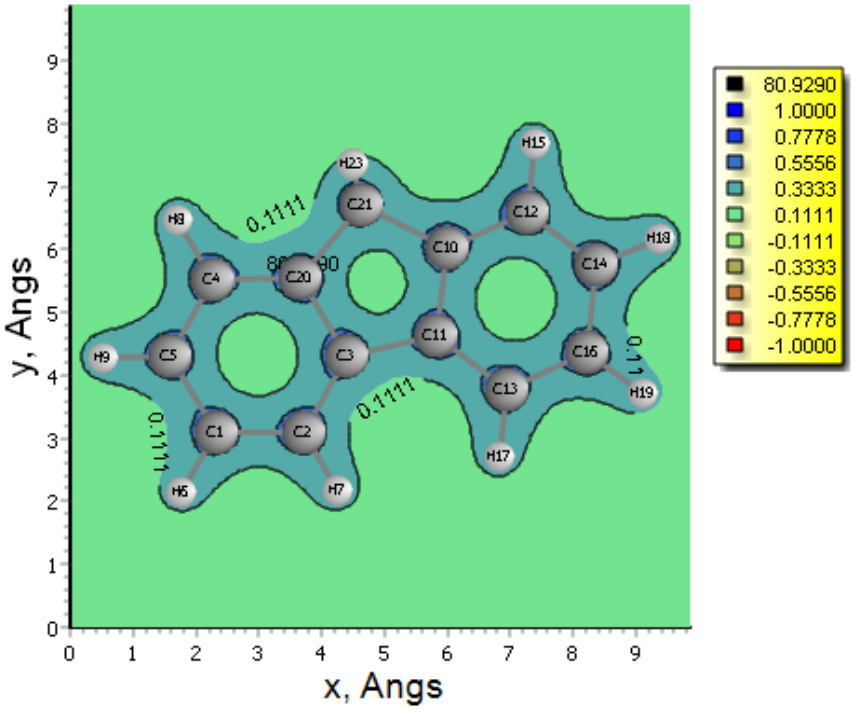

Figure 4.10: 2-D electron density contour map for fluorene calculated using Chemissian

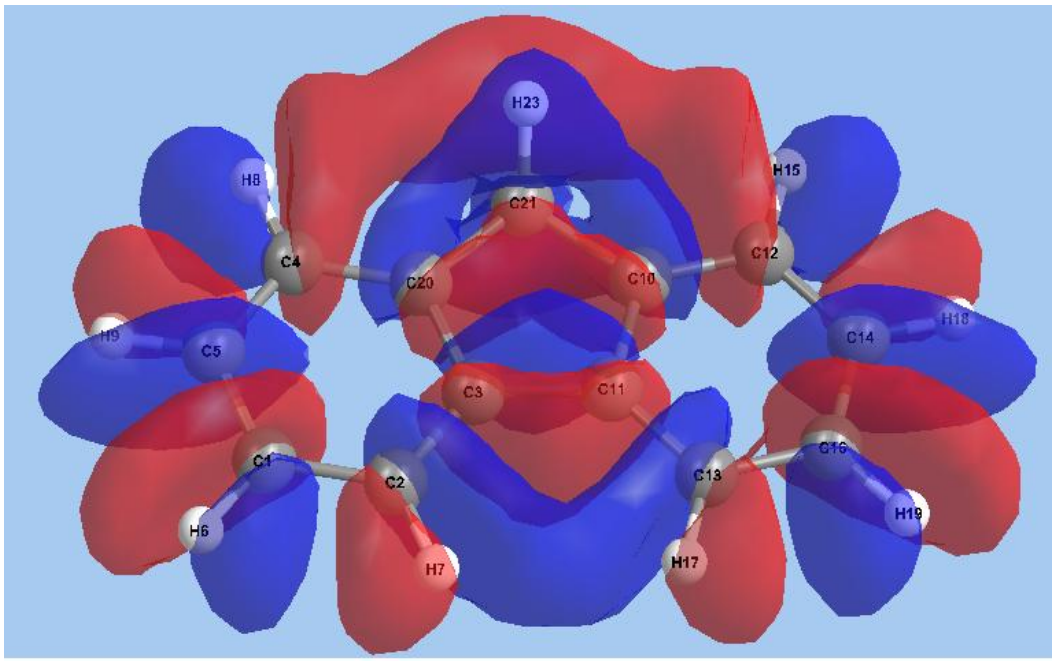

Figure 4.11: 3-D molecular orbital diagram showing electronic density for fluorene at an isovalue of 0.02

Electron density maps are very important in understanding electrophilic and nucleophilic sites. Conventionally, the negative potential sites (red colour) represents regions of electrophilic reactivity and interactions through π–π bonding within aromatic systems and

positive potential sites (blue colour) represents regions of nucleophilic reactivity. These maps are critical in determining regions of high electron density within a molecule. Electron distribution gives insight on the behaviour of a particular toxicant and probably the binding site during reactions with biological structures or tissues.

4.12 Histochemistry

This is the study of the identification and distribution of chemical compounds within and between biological cells using histological techniques such as histology stains, indicators and light (optical) and electron microscopy.

4.12.1 Examination of lung damage by particulate matter

Environmental particulates in the air are a mixture of components like organic chemicals, nitrates, sulphates, metals, soil, and dust particles. Carbon makes up roughly 60% of particulate matter in the air, primarily in the form of organic volatiles and elemental carbon. The elemental carbon, i.e. black carbon, is a major pollutant formed in the combustion process. In general, the surface area of inhaled particulates is more decisive of their toxicity than their size, and smaller particles tend to have a larger relative surface area. Consequently, it is well-known that nano-particulates can penetrate deep into the respiratory tract during breathing and thereby cause significant respiratory problems.

In order to understand the inhalation toxicity of particulates, lungs of albino mice exposed to particulates for six hours/day were examined by a light microscopy interfaced with a computer to assess the effects on the tissues. Figure 4.12 presents the extracted lungs from albino mice exposed to various types of soot particulates.

Figure 4.12: Image **1** is the lung exposed to diesel while **2** is the lung exposed to tyre particulates

After sections of 3~4-µm thick were cut and stained with hematoxylin and eosin (H&E), they were examined histologically. Two exposure-related findings were apparent in comparison to the control lung sample (Figure 4.13A, *vide infra*) i.e.

i. Maximum to mild yellow-brown to black pigmentation within the alveolar macrophages following a 7 day exposure of tyre and 9 days exposure of diesel combustion exhaust.
ii. Minimal increase in alveolar macrophages (histiocytosis) following exposure to simulated forest fire soot.

The alveolar histiocytosis was characterized by slightly increased number of alveolar macrophages that in general were diffusely distributed throughout the lung. The pigmented particulates found in the alveolar macrophages from the recovery animals were more commonly observed in punctate aggregates, possibly reflecting continued cellular processing of the material. Histopathological effects in the lung following exposure to the three combustion sources shows that the control mouse exposed to ambient air for 14 days had normal alveolar air spaces and septa (Figure 4.13 A).

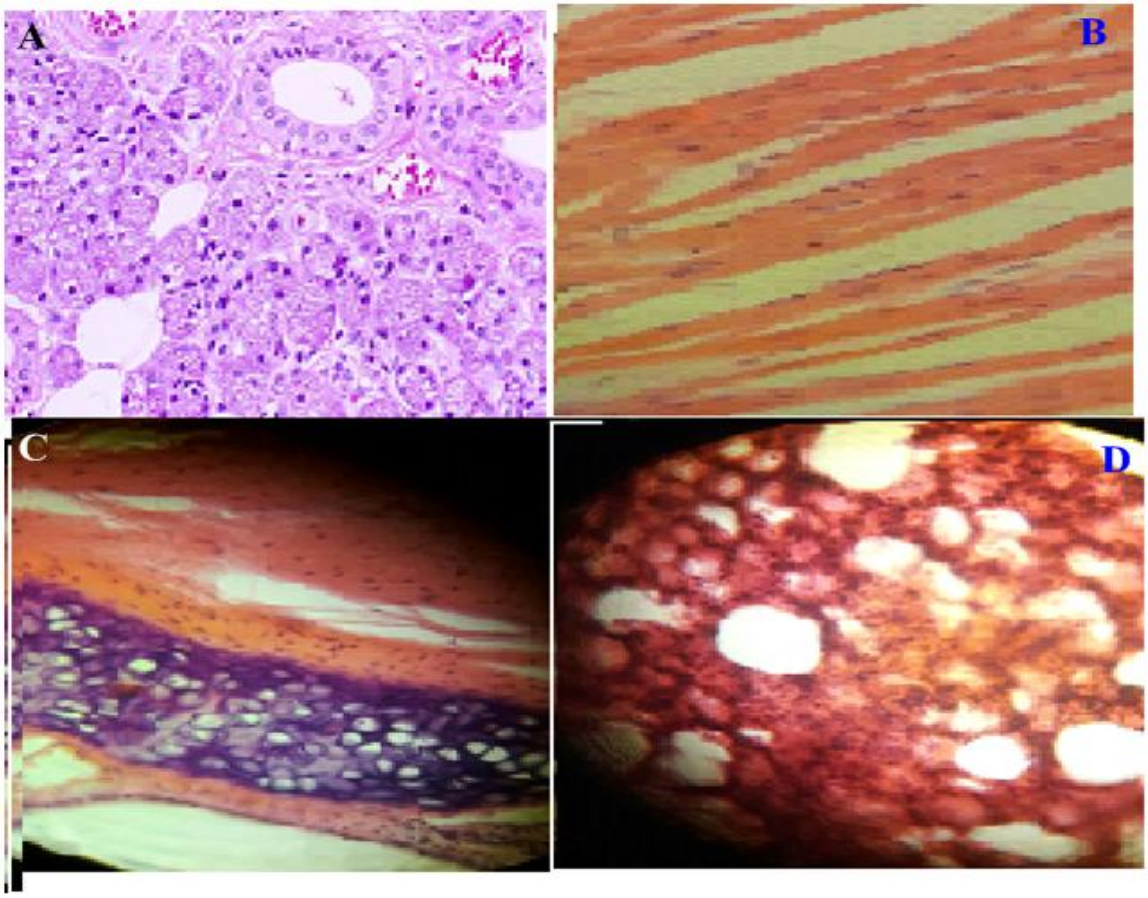

Figure 4.13: Lung tissue photographs obtained from a light microscope at ×200 magnification; **A**-control (non-exposed), **B**- forest fire particulate exposed tissue, **C**- tyre particulate exposed tissues, and **D**–diesel particulate exposed tissue.

Air spaces contain scattered pulmonary interstitial macrophages. The mice exposed to forest fire soot (Figure 4.13B) showed minimally affected airways. However, the mice that were exposed to the diesel soot (Figure 4.13D, died after 9 days of exposure) indicated that alveolar air spaces contained increased macrophages with minimal to mild pigmentation while those exposed to tyre emissions (Figure 4.13C) died after 7 days. Clearly, as observed in Fig. C, pulmonary alveolar macrophages contained dark yellow to black intracytoplasmic pigments. Deposition of soot particulates (black pigments can be noted in Figures 4.13B, C, and D).

4.12.2 Effects of particulate emissions on the lungs tissues of albino mice

This study proposes that soot emissions alone may not be responsible for the observed effects noticed in Figure 4.13B, C and D. Clearly, from the GC-MS data, numerous classes of toxic organic volatiles are also released during the thermal degradation of diesel and tyre samples and may contribute markedly to cell injury, growth of tumors, and eventually death. Nevertheless, soot may also pose serious health impacts probably because of the organic radicals bound to the soot particles. This observation is evident in tyre emissions which accelerated the death of the mouse exposed to it despite few organic volatiles detected in tyre burning in comparison to those detected in combustion of diesel. Although, the GC-MS analysis of simulated forest fire emissions conducted in this study was not substantial, it is possible to extrapolate based on the results of tyre burning that not many organic toxins can be formed from forest fire emissions. Nonetheless organic volatiles from forest fire are the subject of critical discussions in our ongoing studies on fireworks, forest fires, and volcanic fires. The toxicity of organic volatiles especially PAHs are well-documented in literature and will not be discussed further.

The respiratory tract epithelium normally begins at the nostrils and extends to the alveoli. Its cellular composition conventionally varies greatly by function and structural site along the respiratory path. Volatiles carried into the respiratory tract are known to pass over epithelial cells in the nostril (Barile, 2013). These cells represent a natural block whose function is the removal of inhaled foreign substances. They are most likely the primary cells to exhibit the adverse consequences of exposure to inhaled particulates and thereby may serve as a sensitive and direct measure of particle toxicity (Landsiedel *et al.*, 2014) as observed in Figure 4.13C and D, vide *infra*. Epithelial cells lining the tracheobronchial tree, central acini, and alveoli of the lungs also serve as sensitive indicators of the pattern of induced injury due

to soot emissions deposition and subsequent particle-mediated events in these regions. Two important sites for particle deposition in the lungs are the respiratory bronchioles and central acini. These two sites showed significant damage as evidenced in Figure 4.13C. These structures form the transitional zone between the air conduction path and gas exchange alveoli. In mice, the transition from the terminal bronchiole to the alveolar duct is immediate (Townsley, 2012). In contrast, humans possess a more complex transitional zone, with one to three generations of airways. Because the respiratory bronchioles and central acini are primary sites for lung injury after exposure to airborne pollutants (Adamson *et al.*, 1999), it is critical to understand the effects of particle deposition on structural and functional changes in this region (Pinkerton and Joad, 2000).

This study has demonstrated that diesel exhaust inhalation and tyre soot inhalation for a substantial period (i.e. 7 days for tyre and 9 days for the diesel particulate exposure) of time aggravates the neutrophilic lung swelling or proinflammatory chemokine expressions related to lung dysfunction. The mouse exposed to tyre emissions died after a week (7 days) while that exposed to vehicular diesel soot died after 9 days of exposure. On the other hand, the mouse exposed to simulated forest fire soot did not die even after 14 days of continuous exposure although it showed signs of weakening and watery eyes. Nevertheless, the lung pathology observed in the mice following the experimental exposures to the particulate emissions from different fuels (forest fire, tyre, and diesel) showed significant similarities; airway epithelial, necrosis, and parenchymal congestion, edema, hemorrhage and inflammation (Figures 4.13B, C, and D). However, the microscopic examination of lung sections indicated marked differences between the lungs of exposed mice, and the control (Figure 4.13A). A great accumulation of soot particles was found surrounding the bronchioles in the lymphatics, with the surrounding alveolar wall structures frequently absent especially in the tyre particulate and diesel-exposed lungs. This condition is similar anatomically to that of the centrilobular emphysema as reported in literature (Ghio *et al.*, 2000).

Particulate emissions generated by tyre burning exhibited extensive destruction to the tissues. This is because of evident damage to the cells which was significant: capillary disconnection and blockage of air pathways (Figure 4.13C). Exposure of mice to diesel soot particles also impaired cell proliferation in the alveolar region of the lung (Figure 4.13D). Clear evidence of inflammation was observed in all exposures. However, forest fire soot showed minimal damage (Figure 4.13B). Remarkably, in all exposures, the biological response in the airways and lung tissue to inhalation of soot particles was dependent on the source of particulate

emissions. Focal airway epithelial necrosis was found in the trachea and with decreasing frequency distally not noticed in terminal bronchioles. The damage to the endothelium and the alveolar epithelium resulted in the creation of an open interface between the lung and the blood which facilitated the spread of soot particulates from the lung systemically, and ultimately a systemic inflammatory response (Morrison and Bidani, 2002).

It is well established in literature that, the injury to epithelial cells handicaps the ability of the lung to pump fluid out of airspaces (Bhanothu *et al.*, 2012). Fluid filled airspaces, loss of surfactant, micro-vascular thrombosis, and unsystematic repair reduces resting lung volumes, leading to increased ventilation-perfusion discrepancy from right to the left shunt resulting to breathing problems. In addition, lymphatic drainage of lung units appears to be reduced, i.e. dazed by the acute injury which contributes to the build-up of extravascular fluid (Luh and Chiang, 2007). Vessels were markedly congested while in others, vessels were distantly pulled apart (Figures 4.13C and D). Edema was also observed around broncho-vascular trunks, Figures 4.13B, C, and D, *vide supra*. The non-specificity of these changes mostly reflects the direct toxicity of many soot components, the effects of products released from locally altered or reactive inflammatory leucocytes, platelets and endothelial cells and changes in the flow of the lung blood (Morrison and Bidani, 2002). There were more convincing differences between the tyre and diesel exposures, from the fact that the tyre soot caused sudden death (after 7 days) as compared to mouse exposed to diesel soot which died after 9. There was also swelling and shrinking of tissues cells i.e. the tyre and vehicular diesel soot volatiles caused disconnection of the connective tissues and blood capillaries within the lungs, which evidently caused swelling and shrinking as noted in Figures 4,13C and D, *vide supra*.

CHAPTER FIVE

CONCLUSIONS AND RECOMMENDATIONS

5.1 Conclusion

Particulate emissions from simulated forest fire, thermolysis of tyre and diesel were found to yield numerous compounds of diverse classifications; PAHs, long chain hydrocarbons, oxygenated by-products, aromatic compounds and special class of compounds (dibenzo-*p*-dioxin, and 2H-benzopyran). The special class of compounds including dibenzo-*p*-dioxin in presence of small amounts of chlorine and a transition metal such as iron may lead to the formation of the deadliest environmental pollutants referred to as chlorinated dioxins. Therefore, emissions from forest fire can be deadly in their own right. This study has also investigated the mechanistic formation of free radicals from neutral molecular products which are considered injurious to human health and established precursors for cancer, respiratory ill health, and oxidative stress. The formation of isobenzofuran-1, 3-dione from molecular 1, 2-benzene dicarboxylic acid (phthalic acid) as one of the major by-products of forest fire has successfully been elucidated theoretically in this study

The soot particulate size from simulated forest fire and tyre burning were found to be slightly larger than PM_{10} but they are attributed to belong in this class of particulates. These types of particulates may be responsible to alveoli microphage injury, damage to respiratory tract, and other degenerative diseases including aging and whizzing of the lungs. They are capable of penetrating deep into the alveoli of the lungs.

This study has also indicated that exposure to tyre and diesel exhaust particulates have the greatest impact on lung tissues and may cause serious biological ailments to higher order animals such as man. There is also the production of irritant compounds such as PAHs - benzene, benzo[a]pyrene, pyrene, and cyclopentafused PAHs (fluorene and fluoranthene) as reported in this study and literature surveys. These organic toxicants may act as precursors that disrupt the normal lining of the respiratory tract and cause potential swelling, airway collapse, and respiratory distress. Forest fire soot, however, may cause some health effects but requires a longer duration of exposure before the impacts become significant. Moreover, there was a plausible degree of neutrophilic infiltration seen in the lung specimens as a results of exposure to diesel and tyre particulate emissions. Accordingly as reported in literature surveys, exposure to increased ambient amounts of particulate

emissions is associated with an increase in morbidity and daily mortality especially in industrialized cities. A probable biological mechanism linking soot exposure and pathophysiological effects has not been fully established. This study, nevertheless, has proposed that a number of factors may be responsible for ill health occasioned by particulate emissions; exposure to particulate matter, organic volatiles, and radicals which may be bound to particulates

5.2 Recommendations

Although this study has thoroughly investigated the particulate emissions and organic volatiles from common combustion sources (tyre, diesel exhaust, and simulated forest fire), the following recommendations are necessary:

1. There is need to investigate the radical behaviour of intermediates generated during combustion using electron paramagnetic resonance spectroscopy (EPR).
2. Characterization of particulate emissions from diesel would be necessary in order to classify them as either PM_{10} or $PM_{2.5}$.
3. There is need to protect forests from fire outbreaks in order to secure natural habitats, prevents annihilation of food chains and most importantly minimize pollution which could be detrimental to both humans and naturals ecosystems.
4. There is also need of continuous improvement of vehicular engines and use of catalytic converters in exhaust pipes to reduce or prevent emission of harmful particulates in the environment.

REFERENCES

Abdel-Shafy, H., and Mansour, M. (2016). A review on polycyclic aromatic hydrocarbons: source, environmental impact, effect on human health and remediation. *Egyptian Journal of Petroleum, **25***(1), 107-123.

Adamson, I. Y., Vincent, R., and Bjarnason, S. G. (1999). Cell injury and interstitial inflammation in rat lung after inhalation of ozone and urban particulates. *American journal of respiratory cell and molecular biology, **20***(5), 1067-1072.

Akbaba, M., and Kurt, B. (2016). Diesel Exhaust and Cancer. *Turkish Journal of Occupational/Environmental Medicine and Safety, **1***(3).

Andrews, J. E., Brimblecombe, P., Jickells, T. D., Liss, P. S., and Reid, B. (2013). *An introduction to environmental chemistry*: John Wiley & Sons.

Apicella, B., Millan, M., Herod, A., Carpentieri, A., Pucci, P., and Ciajolo, A. (2006). Separation and Measurement of flame-formed high molecular weight polycyclic aromatic hydrocarbons by size-exclusion chromatography and laser desorption/ionization TOF mass spectrometry. *Rapid commun. Mass spectrom, **20***.

Appel, J., Bockhorn, H., and Frenklach, M. (2000). Kinetic modeling of soot formation with detailed chemistry and physics: laminar premixed flames of C_2 hydrocarbons. *Combustion and Flame, **121***(1–2), 122-136.

Bachmann, M., Wiese, W., and Homann, K. (1996). *PAH and aromers: precursors of fullerenes and soot.* Paper presented at the Symposium (International) on Combustion.

Baker, R. R., Coburn, S., and Liu, C. (2006). The pyrolytic formation of formaldehyde from sugars and tobacco. *Journal of Analytical and Applied Pyrolysis, **77***(1), 12-21.

Barfknecht, T. R. (1983). Toxicology of soot. *Progress in Energy and Combustion Science, **9***(3), 199-237.

Barile, F. A. (2013). *Principles of toxicology testing*: CRC Press.

Bates, J. T., Weber, R. J., Abrams, J., Verma, V., Fang, T., Klein, M., Strickland, M. J., Sarnat, S. E., Chang, H. H., and Mulholland, J. A. (2015). Reactive oxygen species generation linked to sources of atmospheric particulate matter and cardiorespiratory effects. *Environmental science & technology, **49***(22), 13605-13612.

Baulig, A., Garlatti, M., Bonvallot, V., Marchand, A., Barouki, R., Marano, F., and Baeza-Squiban, A. (2003). Involvement of reactive oxygen species in the metabolic pathways triggered by diesel exhaust particles in human airway epithelial cells. *Am J Physiol Lung Cell Mol Physiol, **285***, L671–L679.

Bauschlicher, J., Charles, W., and Ricca, A. (2000). Mechanisms for polycyclic aromatic hydrocarbon (PAH) growth. *Chemical Physics Letters, **326***(3), 283-287.

Bejaoui, S., Batut, S., Therssen, E., Lamoureux, N., Desgroux, P., and Liu, F. (2015). Measurements and modeling of laser-induced incandescence of soot at different heights in a flat premixed flame. *Applied Physics B, **118***(3), 449-469.

Berdahl, P., Akbari, H., Levinson, R., and Miller, W. A. (2008). Weathering of roofing materials – An overview. *Construction and Building Materials, **22***(4), 423-433.

Bergethon, P. R. (2013). *The physical basis of biochemistry: the foundations of molecular biophysics*: Springer Science & Business Media.

Bhanothu, V., Theophilus, J., Rozati, R., Badhini, P., Vijayalaxmi, B., and Reddy, K. (2012). Review on Recent Aspects of Biochemical, Cellular, Physiological Markers and Environmental Factors Associated with Acute Lung Inflammation & Injury (ALI). *American Journal of Biochemistry, **2***(5), 74-88.

Bogarra, M., Herreros, J., Tsolakis, A., York, A., and Millington, P. (2016). Study of particulate matter and gaseous emissions in gasoline direct injection engine using on-board exhaust gas fuel reforming. *Applied Energy, **180***, 245-255.

Bølling, A. K., Pagels, J., Yttri, K. E., Barregard, L., Sallsten, G., Schwarze, P. E., and Boman, C. (2009). Health effects of residential wood smoke particles: the importance of combustion conditions and physicochemical particle properties. *Particle and fibre toxicology, **6***(1), 1.

Bolton, J. L., Trush, M. A., Penning, T. M., Dryhurst, G., and Monks, T. J. (2000). Role of quinones in toxicology. *Chemical Research in Toxicology, **13***(3), 135-160.

Brook, R. D., Rajagopalan, S., Pope, C. A., Brook, J. R., Bhatnagar, A., Diez-Roux, A. V., Holguin, F., Hong, Y., Luepker, R. V., and Mittleman, M. A. (2010). Particulate matter air pollution and cardiovascular disease an update to the scientific statement from the American Heart Association. *Circulation, **121***(21), 2331-2378.

Brunekreef, B., and Forsberg, B. (2005). Epidemiological evidence of effects of coarse airborne particles on health. *European Respiratory Journal, **26***(2), 309-318.

Bruno, A., Lisio, C., Galla, D., Min-utolo, P., and D'Alessio, A. (2002). Specroscopy of engines and flame produced nano organic compounds suspended in water. *in proc.29th symp(int) on combustion*.

Calcote, H. F. (1981). Mechanisms of soot nucleation in flames—A critical review. *Combustion and Flame, **42***, 215-242.

Chaturvedi, K. (2010). Aviation Combustion Toxicology. *Analytical Toxicology, **34***, 3-16.

Chen, Y. H., Bakrania, S. D., Wooldridge, M. S., and Sastry, A. M. (2010). Image Analysis and Computer Simulation of Nanoparticle Clustering in Combustion Systems. *Aerosol Science and Technology, **44***(1), 83-95.

Cheng, T., Wu, Y., Gu, X., and Chen, H. (2015). Effects of mixing states on the multiple-scattering properties of soot aerosols. *Optics express, **23***(8), 10808-10821.

Chung, S. (2011). *Computational modeling of soot nucleation.* University of Michigan.

Crittenden, B., and Long. (1973). Formation of Polycyclic aromatic hydrocarbons in rich premixed acetylene and ethylene flames. *combust flame*(37), 359.

D'Anna, A., D'Alessio, A., Minutolo, P., and Bockhorn, H. (1994). Soot Formation in Combustion: Mechanisms and Models. *H. Bockhorn, Springer-Verlag, Heidelberg*, 83.

Dagaut, P., Voisin, D., Cathonnet, M., McGuinness, M., and Simmie, J. M. (1996). The oxidation of ethylene oxide in a jet-stirred reactor and its ignition in shock waves. *Combustion and Flame, **106***(1-2), 62-68.

Delfino, R. J., Sioutas, C., and Malik, S. (2005). Potential role of ultrafine particles in associations between airborne particle mass and cardiovascular health. *Environmental health perspectives*, 934-946.

Dellinger, B., Pryor, W., Cueto, R., Squadrito, G. L., Hegde, V., and Deutsch, W. A. (2001). Role of free radicals in the toxicity of airborne fine particulate matter. *Chemical Research in Toxicology, **14***(10), 1371-1377.

Dellinger, B., Pryor, W. A., Cueto, R., Squadrito, G., and Deutsch, W. A. (2000). The role of combustion-generated radicals in the toxicity of $PM_{2.5}$. *Proceedings of the Combustion Institute, **28***, 2675-2681.

Dellinger, B., WA.Pryor, Cueto, R., Squadrito, G., Hegde, V., and Deutsch, W. (2001). Role of free radicals in the toxicity of airborne fine particulate matter. *Chem Res Toxicol, **14***, 1371-1377.

Ding, K., Zhong, Z., Zhang, B., Song, Z., and Qian, X. (2015). Pyrolysis characteristics of waste tire in an analytical pyrolyzer coupled with gas chromatography/mass spectrometry. *Energy & Fuels, **29***(5), 3181-3187.

Dobbins, R., and Subramaniasivam, H. (1994). Soot precursor particles in flame. Soot Formation in Combustion-Mechanisms and Models. (Vol. 290, pp. 19-32). Bockhorn H: Berlin: Springer Verlag.

Dong, J., Zhao, J. M., and Liu, L. H. (2015). Morphological effects on the radiative properties of soot aerosols in different internally mixing states with sulfate. *Journal of Quantitative Spectroscopy and Radiative Transfer, **165***, 43-55.

Downard, J., Singh, A., Bullard, R., Jayarathne, T., Rathnayake, C. M., Simmons, D. L., Wels, B. R., Spak, S. N., Peters, T., and Beardsley, D. (2015). Uncontrolled combustion of shredded tires in a landfill–Part 1: Characterization of gaseous and particulate emissions. *Atmospheric Environment, **104***, 195-204.

Edwards, D. E., Zubarev, D. Y., Lester, W. A., Jr., and Frenklach, M. (2014). Pathways to soot oxidation: reaction of OH with phenanthrene radicals. *J Phys Chem A, **118***(37), 8606-8613.

Eggersdorfer, M. L., and Pratsinis, S. E. (2013). Restructuring of aggregates and their primary particle size distribution during sintering. *AIChE Journal, **59***(4), 1118-1126.

Evans, C. S., and Dellinger, B. (2003). Mechanisms of dioxin formation from the high-temperature pyrolysis of 2-bromophenol. *Environmental Science & Technology, **37***(24), 5574-5580.

Evans, C. S., and Dellinger, B. (2005). Mechanisms of dioxin formation from the high-temperature oxidation of 2-bromophenol. *Environmental Science & Technology, **39***(7), 2128-2134.

Fahlman, B. D. (2011). Nanomaterials *Materials Chemistry* (pp. 457-583): Springer

Forbes, P., and Garland, R. (2016). Outdoor Air Pollution. *Comprehensive Analytical Chemistry*.

Frenklach, M. (2002). Reaction mechanism of soot formation in flames. *Phys. Chem., **4***, 2028-2037.

Frenklach, M., Clary, W., Gardiner, W., and Stein, S. (1985). Detailed Kinetic Modeling of Soot Formation in Shock-Tube Pyrolysis of Acetylene. *Symposium (International) on Combustion, **20***(1), 887-901.

Frenklach, M., and Ping, J. (2004). On the role of surface migration in the growth and structure of graphene layers. *Carbon, **42***(7), 1209-1212.

Frenklach, M., Taki, S., Durgaprasad, M., and Matula, R. (1983). A Conceptual Model for Soot Formation in Pyrolysis of Aromatic Hydrocarbons. *Combust. Flame, **49***, 275-282.

Frenklach, M., and Wang, H. (1991). Detailed reduction of reaction mechanisms for flame modeling. *Combustion and Flame, **87***(3), 365-370.

Frenklach, M., and Wang, H. (1994a). Detailed Mechanism and Modeling of Soot Particle Formation. In H. Bockhorn (Ed.), *Soot Formation in Combustion* (Vol. 59, pp. 165-192): Springer Berlin Heidelberg

Frenklach, M., and Wang, H. (1994b). Soot Formation in Combustion. *Mechanisms and Models*, p. 165.

Frenklach, M., and Warnatz, J. (1987). Detailed Modeling of PAH Profiles in a Sooting Low-Pressure Acetylene Flame. *Combust. Sci. Technol.*, ***51***, 265-283.

Frenklach., M., Nigel W. (1998). Hydrogen migration in polyaromatic growth. *Symposium (International) on Combustion*, ***27***(2), 1655-1661.

Friedlander, S. K. (2000). *Fundamentals of Aerosols Dynamics*. oxford,New York: Oxford University Press.

Frisch, M. J., Trucks, G., Schlegel, H., Scuseria, G., Robb, M., Cheeseman, J., Scalmani, G., Barone, V., Mennucci, B., and Petersson, G. (2009). Gaussian 09, revision A. 1. *Gaussian Inc., Wallingford, CT*.

Gad, S. C. (1990). The toxicity of smoke and combustion gases. *In Combustion Toxicology*, 63-80.

Gaffney, J. S., Marley, N. A., and Smith, K. J. (2015). Characterization of fine mode atmospheric aerosols by Raman microscopy and diffuse reflectance FTIR. *The Journal of Physical Chemistry A*, ***119***(19), 4524-4532.

García-Pérez, J., Morales-Piga, A., Gómez, J., Gómez-Barroso, D., Tamayo-Uria, I., Romaguera, E. P., Fernández-Navarro, P., López-Abente, G., and Ramis, R. (2016). Association between residential proximity to environmental pollution sources and childhood renal tumors. *Environmental research*, ***147***, 405-414.

Geiser, M., Rothen-Rutishauser, B., kapp, N., Schurch, S., Kreyling, W., Schultz, H., Semmler, M., Im Hof, V., Heyder, J., and Gehr, P. (2005). Ultrafine particles cross cellular membranes by nonphagocytotic mechanisms in lungs and in cultured cells Environ. *Health Perspect.*, ***113***, 1555-1560.

Gelbard, F., and Seinfeld, J. H. (1980). Simulation of Multicomponent Aerosol Dynamics. *Journal of Colloid and Interface Science,*, ***78***, 485-501.

Ghio, J., Kim, C., and Devlin, R. (2000). Concentrated ambient air particles induce mild pulmonary inflammation in healthy human volunteers. *American journal of respiratory and critical care medicine*, ***162***(3), 981-988.

Guidotti, T. L. (2016). Toxic Hazards *Health Risks and Fair Compensation in the Fire Service* (pp. 63-92): Springer

Gwaze, P., Schmid, O., Annegarn, H., Andreae, M., Huth, J., and Helas, G. (2006). Comparison of three methods of fractal analysis applied to soot aggregates from wood combustion. *J Aerosol Sci* ***37***, 820-838.

Haynes, B. S., and Wagner, H.G.. (1981). Soot formation. *Prog. Energy Combust.Sci.*, ***7*** (229).

Helen, J. P., and Paulson, E. P. (1997). Reactive Oxygen Species and Antioxidants in Signal Transduction and Gene Expression. *Lead Review Article*, 353-361.

Henning, R., and Howard, J. (2000). Formation of polycyclic aromatic hydrocarbons and their growth to soot—a review of chemical reaction pathways. *Progress in Energy and Combustion science*, ***26***(4), 565-608.

Higgins, K., Jung, H., Kittelson, B., Roberts, T., and Zachariah, R. (2002). Size-selected nanoparticle chemistry: Kinetics of soot oxidation. *The Journal of Physical Chemistry A*, ***106***(1), 96-103.

Howard, J., and Longwell, P. (1983). *Formation Mechanisms of PAH and Soot in Flames*. Paper presented at the 7th Int. Symp. Polynuclear Aromatic Hydrocarbons: Formation, Metabolism, and Measurement, Columbus, Ohio.

Huang, H., Zhou, C., Liu, Q., Wang, Q., and Wang, X. (2016). An experimental study on the combustion and emission characteristics of a diesel engine under low temperature combustion of diesel/gasoline/n-butanol blends. *Applied Energy*, ***170***, 219-231.

Hudda, N., and Fruin, S. (2016). International Airport Impacts to Air Quality: Size and Related Properties of Large Increases in Ultrafine Particle Number Concentrations. *Environmental science & technology*, ***50***(7), 3362-3370.

IARC, I. A. f. R. o. C. (2005). *IARC handbooks of cancer prevention* (Vol. 10): IARC.

Indarto, A. (2008). Soot Growth Mechanisms from Polyynes. *Environmental Engineering Science*, ***26***(12), 1685-1691.

Indarto, A. (2009). Soot Growth Mechanisms from Polyynes. *Environmental Engineering Science*, ***26***(12).

Jayaraman, A., Beig, G., Kulshrestha, U., Lahiri, T., Ray, M., Satheesh, S., Sharma, C., and Venkataraman, C. (2010). Atmospheric Composition Change and Air Quality *Global Environmental Changes in South Asia* (pp. 171-221): Springer

Jorg, A., Bockhorn, H., and Frenklach, M. (2000). Kinetic modeling of soot formation withdetailed chemistry and physics: laminar premixed flames of C_2 hydrocarbons. *Combust and Flame, **121***, 122-136.

Junjie, H., Huimin, M., Wenbing, Z., Zhiqing, Y., Guoying, S., and Fu, J. (2014). Effects of Benzene and Its Metabolites on Global DNA Methylation in Human Normal Hepatic L02 Cells. *Environ Toxicol, **29***, 108-116.

Kamens, M., Guo., Z., Fulcher, J. N., and Bell, A. (1988). The influence of humidity, sunlight, and temperature on the daytime decay of polyaromatic hydrocarbons on atmospheric soot particles. *Environmental Science & Technology, **22***(1), 103-108.

Kazakov, H., Wang, H., and Frenklach, M. (1995). Detailed Modeling of Soot Formation in Laminar Premixed Ethylene Flames at a Pressure of 10 Bar. *Combust. Flame, **100***, 111-120.

Kelly, F. J., and Fussell, J. C. (2012). Size, source and chemical composition as determinants of toxicity attributable to ambient particulate matter. *Atmospheric environment, **60***, 504-526.

Kenley, P., Loren, G., Gergely, G., and Mazziotti, D. (2011). Strong Correlation in Acene Sheets from the Active-Space Variational Two-Electron Reduced Density Matrix Method: Effects of Symmetry and Size. *Physical Chemistry*.

Khosousi, A., and Benjamin, S. (2015). Detailed modeling of soot oxidation by oxygen and OH in laminar difusion flames. *Combustion, **35***(2), 1903-1910.

Kibet, J., Khachatryan, L., and Dellinger, B. (2012). Molecular Products and Radicals from Pyrolysis of Lignin. *Environmental Science & Technology, **46***(23), 12994-13001.

Kibet, J., Khachatryan, L., and Dellinger, B. (2013). Molecular products from the pyrolysis and oxidative pyrolysis of tyrosine. *Chemosphere, **91***(7), 1026-1034.

Kibet, J., Khachatryan, L., and Dellinger, B. (2015). Phenols from pyrolysis and co-pyrolysis of tobacco biomass components. *Chemosphere, **138***, 259-265.

Kimwele, C., Matheka, D., and Ferdowsian, H. (2011). A Kenyan perspective on the use of animals in science education and scientific research in Africa and prospects for improvement. *Pan African Medical Journal, **9***(1).

Ko, F. W., and Hui, D. S. (2012). Air pollution and chronic obstructive pulmonary disease. *Respirology, **17***(3), 395-401.

Köhler, C., and Allgeier, T. (2015). Exhaust emissions *Gasoline Engine Management* (pp. 260-267): Springer

Koylu, U. O., and Faeth, G. M. (1992). Structure of overfire soot in buoyant turbulent diffusion flames at long residence times. *journal of Combust Flame, **89***(2), 140-156.

Krestinin, A. V. (1998). Formation of soot particles as aprocess involving chemicalcondensation of polyenes.

Kreyling, W. G., Möller, W., Semmler-Behnke, M., Oberdörster, G., Donaldson, K., and Borm, P. (2007). Particle dosimetry: deposition and clearance from the respiratory tract and translocation towards extrapulmonary sites. *Particle toxicology*, 48-69.

Kreyling, W. G., Semmler-Behnke, M., and Möller, W. (2006). Ultrafine particle-lung interactions: does size matter? *Journal of Aerosol Medicine, **19***(1), 74-83.

Kugler, L., Salaneck, William R. (1999). Photoelectron Spectroscopy and Quantum Chemical Modeling Applied to Polymer Surfaces and Interfaces in Light-Emitting Devices. *Accounts of Chemical Research, **32***(3), 225-234.

Labota, J., Kaats-Richter, V., Kopera, C., Vlietstraa, J., W.A., R., Leonardus, W., and Seinenc, W. (2005). CP-arene oxides: the ultimate, active mutagenic forms of cyclopenta-fused polycyclic aromatic hydrocarbons (CP-PAHs). *Mutation Research, **581***, 115–132.

Landsiedel, R., Sauer, U. G., Ma-Hock, L., Schnekenburger, J., and Wiemann, M. (2014). Pulmonary toxicity of nanomaterials: a critical comparison of published in vitro assays and in vivo inhalation or instillation studies. *Nanomedicine, **9***(16), 2557-2585.

Lautenberger, C. W., de Ris, J. L., Dembsey, N. A., Barnett, J. R., and Baum, H. R. (2005). A simplified model for soot formation and oxidation in CFD simulation of non-premixed hydrocarbon flames. *Fire Safety Journal, **40***(2), 141-176.

Lenoid, S. (2012). Chemissian (Version 3.3). Retrieved from http://www.chemissian.com/.2012

Li, N., Xia, T., and Nel, A. E. (2008). The role of oxidative stress in ambient particulate matter-induced lung diseases and its implications in the toxicity of engineered nanoparticles. *Free Radical Biology and Medicine, **44***(9), 1689-1699.

Lin, Q., Ye, Q., Deng, H., and Zhang, X. (2008). Field analysis of acetaldehyde in mainstream tobacco smoke using solid-phase microextraction and a portable gas chromatograph. *Journal of Chromatography A, **1198***, 34-37.

Lippmann, M., and Schlesinger, R. (2000). Toxicological bases for the setting of health-related air pollution standards. *Annual review of public health, **21***(1), 309-333.

Liu, F., Karataş, A. E., Gülder, Ö. L., and Gu, M. (2015). Numerical and experimental study of the influence of CO_2 and N_2 dilution on soot formation in laminar coflow C_2H_4/air diffusion flames at pressures between 5 and 20 atm. *Combustion and Flame*, ***162***(5), 2231-2247.

Liu., Guo, H., Smallwood, J., and G¨ulder, L. (2001). The chemical effect of carbon dioxide as an additive in an ethylene diffusion flame: implications for soot and NO_x formation. Combust. Flame. *Combust. Flame.*, ***125***, 778–787.

Luh, P., and Chiang, C. (2007). Acute lung injury/acute respiratory distress syndrome (ALI/ARDS): the mechanism, present strategies and future perspectives of therapies. *J Zhejiang Univ Sci*, ***8***, 60-69.

Mansurov, Z. A. (2005). Soot Formation in Combustion Processes (Review). *Combustion, Explosion, and Shock Waves*, ***41***(6), 727-744.

Marcazzan, G. M., Vaccaro, S., Valli, G., and Vecchi, R. (2001). Characterisation of PM10 and PM2. 5 particulate matter in the ambient air of Milan (Italy). *Atmospheric Environment*, ***35***(27), 4639-4650.

Maricq, M. M. (2007). Chemical characterization of particulate emissions from diesel engines: A review. *Journal of Aerosol Science*, ***38***(11), 1079-1118.

Maskos, Z., Khachatryan, L., and Dellinger, B. (2008). Formation of the persistent primary radicals from the pyrolysis of tobacco. *Energy & Fuels*, ***22***(2), 1027-1033.

May, A. A., Saleh, R., Hennigan, C. J., Donahue, N. M., and Robinson, A. L. (2012). Volatility of organic molecular markers used for source apportionment analysis: measurements and implications for atmospheric lifetime. *Environmental science & technology*, ***46***(22), 12435-12444.

May, P., Harvey, J. N., Allan, N., Richley, J., and Mankelevich, Y. A. (2010). Simulations of chemical vapor deposition diamond film growth using a kinetic Monte Carlo model. *Journal of Applied Physics*, ***108***(1), 014905.

McIntosh, J., and Russell, K. (2014). Role of hydrogen abstraction acetylene addition mechanisms in the formation of chlorinated naphthalenes. 1. A quantum chemical investigation. *The Journal of Physical Chemistry A*, ***118***(51), 12192-12204.

Megaridis, C. M., and Dibbins, R. A. (1990). Morphological Description of Flame-Generated Materials. *Combustion Science and Technology*, ***71***, 95-109.

Mehta, R. S. (2008). *Detailed Modeling of Soot Formation and Turbulance-Radiation Interactions.*

Miller, H. J. (1991). Soot Combustion. In p. c. inst (Ed.), (23 ed., pp. 1461)

Mirowsky, J., Hickey, C., Horton, L., Blaustein, M., Galdanes, K., Peltier, R. E., Chillrud, S., Chen, L. C., Ross, J., and Nadas, A. (2013). The effect of particle size, location and season on the toxicity of urban and rural particulate matter. *Inhalation toxicology, **25***(13), 747-757.

Moridani, M. Y., Siraki, A., Chevaldina, T., Scobie, H., and O'Brien, P. J. (2004). Quantitative structure toxicity relationships for catechols in isolated rat hepatocytes. *Chemico-Biological Interactions, **147***(3), 297-307.

Morrison, R., and Bidani, A. (2002). Acute respiratory distress syndrome epidemiology and pathophysiology. *Chest Surg Clin N Am., **12***, 301-323.

Murphy, J., Rouse, R., Polk, W., Henk, G., Barker, A., Boudreaux, J., Floyd, Z., and Penn, A. (2008). Combustion-derived hydrocarbons localize to lipid droplets in respiratory cells. *American Journal of Respiratory Cell and Molecular Biology, **38***(5), 532-540.

Nganai, S., Lomnicki, S., and Dellinger, B. (2012). Formation of PCDD/Fs from oxidation of 2-monochlorophenol over an Fe_2O_3/silica surface. *Chemosphere, **88***(3), 371-376.

Noël, A., Xiao, R., Perveen, Z., Zaman, H., Rouse, R., Paulsen, D., and Penn, A. (2016). Incomplete lung recovery following sub-acute inhalation of combustion-derived ultrafine particles in mice. *Particle and fibre toxicology, **13***(1), 1.

Norinaga, K., and Deutschmann, O. (2007). Detailed Kinetic Modeling of Gas-Phase Reactions in the Chemical Vapor Deposition of Carbon from Light Hydrocarbons. *Ind. Eng. Chem. Res., **46***.

O'Connor, G. T., Neas, L., Vaughn, B., Kattan, M., Mitchell, H., Crain, E. F., Evans, R., Gruchalla, R., Morgan, W., and Stout, J. (2008). Acute respiratory health effects of air pollution on children with asthma in US inner cities. *Journal of Allergy and Clinical Immunology, **121***(5), 1133-1139. e1131.

O'Dowd, C. D., Aalto, P., Hameri, K., Kulmala, M., and Hoffmann, T. (2002). Atmosphereic particles from organic vapours. *Nature (London), **416***, 497.

Oberdörster, G., Oberdörster, E., and Oberdörster, J. (2005). Nanotoxicology: an emerging discipline evolving from studies of ultrafine particles. *Environ. Health. Perspect., **113***, 823-839.

Orasche, J., Seidel, T., Hartmann, H., Schnelle-Kreis, J., Chow, J., Ruppert, H., and Zimmermann, R. (2012). Comparison of emissions from wood combustion. Part 1: Emission factors and characteristics from different small-scale residential heating

appliances considering particulate matter and polycyclic aromatic hydrocarbon (PAH)-related toxicological potential of particle-bound organic species. *Energy & Fuels, **26***(11), 6695-6704.

Palmer, H. B., and Cullis, C. F. (1965). *Chemistry and Physics of Carbon* (M. D. P. L. Walker, New York Ed.).

Pardo, M., Shafer, M. M., Rudich, A., Schauer, J. J., and Rudich, Y. (2015). Single exposure to near roadway particulate matter leads to confined inflammatory and defense responses: Possible role of metals. *Environmental Science & Technology, **49***(14), 8777-8785.

Parr, C., and Pariser, R. (2013). Structure Theory. *Concepts and Methods in Modern Theoretical Chemistry: Electronic Structure and Reactivity, **431***.

Paulik, L. B., Donald, C. E., Smith, B. W., Tidwell, L. G., Hobbie, K. A., Kincl, L., Haynes, E. N., and Anderson, K. A. (2016). Emissions of Polycyclic Aromatic Hydrocarbons from Natural Gas Extraction into Air. *Environmental Science & Technology, **50***(14), 7921-7929.

Pease, C., Rücker, T., and Birk, T. (2016). Review of the Evidence from Epidemiology, Toxicology, and Lung Bioavailability on the Carcinogenicity of Inhaled Iron Oxide Particulates. *Chemical research in toxicology, **29***(3), 237-254.

Perez-Padilla, R., Schilmann, A., and Riojas-Rodriguez, H. (2010). Respiratory health effects of indoor air pollution [Review article]. *The International Journal of Tuberculosis and Lung Disease, **14***(9), 1079-1086.

Perez, G., Cristalli, A., and Lilla, E. (1991). Pyrolysis of benzene-naphthalene mixtures. *Chemosphere, **22***(3–4), 279-284.

Pey, J., Querol, X., Alastuey, A., Rodríguez, S., Putaud, J. P., and Van Dingenen, R. (2009). Source apportionment of urban fine and ultra-fine particle number concentration in a Western Mediterranean city. *Atmospheric Environment, **43***(29), 4407-4415.

Pinkerton, K. E., and Joad, J. P. (2000). The mammalian respiratory system and critical windows of exposure for children's health. *Environmental health perspectives, **108***(Suppl 3), 457.

Pope, C., Burnett, R., Thun, M., Valle, E., Krewski, D., Ito, K., and Thurston, G. (2002). Lung cancer, cardiopulmonary mortality, and long-term exposure to fine particulate air pollution. *J. Amer. Med. Assoc. (JAMA)*(287).

Puri, R., Richardson, T., Santoro, R., and Dobbins, R. (1993). Aerosol dynamic processes of soot aggregates in a laminar ethene diffusion flame. *Combustion and Flame*, ***92***(3), 320-333.

Reddy, M., De, A., and Yadav, R. (2015). Effect of precursors and radiation on soot formation in turbulent diffusion flame. *Fuel*, ***148***, 58-72.

Rengasamy, A., Barger, M., Kane, E., Ma, J., Castranova, V., and Ma, J. (2003). Diesel exhaust particle-induced alterations of pulmonary phase I and phase II enzymes of rats. *Toxicol Environ Health* ***66***, 153–167.

Richter, H., Granata, S., Green, W. H., and Howard, J. B. (2005). Detailed modeling of PAH and soot formation in a laminar premixed benzene/oxygen/argon low-pressure flame. *Proceedings of the Combustion Institute*, ***30***(1), 1397-1405.

Richter, H., and Howard, J. B. (2000). Formation of polycyclic aromatic hydrocarbons and their growth to soot—a review of chemical reaction pathways. *Progress in Energy and Combustion Science*, ***26***(4–6), 565-608.

Robjohns, S., Morris, J., and Verne, J. (2015). Environmental or Toxicological Research. *Chemical Hazards and Poisons Report*, 23.

Saarikoski, S., Timonen, H., Saarnio, K., Aurela, M., Järvi, L., Keronen, P., Kerminen, V., and Hillamo, R. (2008). Sources of organic carbon in fine particulate matter in northern European urban air. *Atmos. Chem. Phys*, ***8***(20), 6281-6295.

Saffaripour, M., Chan, T. W., Liu, F., Thomson, K. A., Smallwood, G. J., Kubsh, J., and Brezny, R. (2015). Effect of Drive Cycle and Gasoline Particulate Filter on the Size and Morphology of Soot Particles Emitted from a Gasoline-Direct-Injection Vehicle. *Environmental science & technology*, ***49***(19), 11950-11958.

Saron, C., Ge´rald, M., Viktorya, A., and Manuel, F. R. (2008). Deamidation of Asparagine Residues: Direct Hydrolysis versus Succinimide-Mediated Deamidation Mechanisms. *J. Phys. Chem. A*, ***113***(6), 1111–1120.

Saunders, K. J. (2013). *Organic polymer chemistry: an introduction to the organic chemistry of adhesives, fibres, paints, plastics, and rubbers*: *Springer Science & Business Media*.

Schwarze, P., Øvrevik, J., Låg, M., Refsnes, M., Nafstad, P., Hetland, R., and Dybing, E. (2006). Particulate matter properties and health effects: consistency of epidemiological and toxicological studies. *Human & Experimental Toxicology*, ***25***(10), 559-579.

Sexton, K., Linder, S. H., Marko, D., Bethel, H., and Lupo, P. J. (2007). Comparative assessment of air pollution-related health risks in Houston. *Environmental Health Perspectives*, 1388-1393.

Sharma, R. K., and Hajaligol, M. R. (2003). Effect of pyrolysis conditions on the formation of polycyclic aromatic hydrocarbons (PAHs) from polyphenolic compounds. *Journal of Analytical and Applied Pyrolysis,*, ***66***, 123-144.

Shaw, G. R., and Connell, D. W. (1994). Prediction and monitoring of the carcinogenicity of polycyclic aromatic compounds (PACs). *Rev Environ Contam Toxicol*, ***135***, 1-62.

Siddens, L. K., Larkin, A., Krueger, S. K., Bradfield, C. A., Waters, K. M., Tilton, S. C., Pereira, C. B., Löhr, C. V., Arlt, V. M., and Phillips, D. H. (2012). Polycyclic aromatic hydrocarbons as skin carcinogens: comparison of benzo [a] pyrene, dibenzo [def, p] chrysene and three environmental mixtures in the FVB/N mouse. *Toxicology and applied pharmacology*, ***264***(3), 377-386.

Sidney, D. N., and Pearson, P. G. (1990). Covalent and non co v alent interactions in acute lethal cell injury caused by chemicals. *Annu. Rev. Pharmacol. Toxicol*, ***30***, 169-195.

Siegmann, K. S., K., andSiegmann,H.C. (2002). Clustering at high temperature; carbon formation in combustion. *Elect. Spect and Related Phenom*, ***126***(121).

Silverman, L. (2012). *Particle size analysis in industrial hygiene*: Elsevier.

Singh, R. I., Mebel, A. M., and Frenklach, M. (2015). Oxidation of graphene-edge six-and five-member rings by molecular oxygen. *The Journal of Physical Chemistry A*, ***119***(28), 7528-7547.

Thomas, R., Vigerstad, T., Meagher, J., and McMullin, C. (2000). Particulate Exposure During the Persian Gulf War. *Occupational Exposure to Carbon Black*(26).

Thurston, G. D., Ahn, J., Cromar, K. R., Shao, Y., Reynolds, H. R., Jerrett, M., Lim, C. C., Shanley, R., Park, Y., and Hayes, R. B. (2016). Ambient particulate matter air pollution exposure and mortality in the NIH-AARP diet and health cohort. *Environmental Health Perspectives*, ***124***(4), 484.

Tilton, S. C., Siddens, L. K., Krueger, S. K., Larkin, A. J., Löhr, C. V., Williams, D. E., Baird, W. M., and Waters, K. M. (2015). Mechanism-based classification of PAH mixtures to predict carcinogenic potential. *Toxicological Sciences*, ***146***(1), 135-145.

Tomczak, A., Miller, A. B., Weichenthal, S. A., To, T., Wall, C., van Donkelaar, A., Martin, R. V., Crouse, D. L., and Villeneuve, P. J. (2016). Long-term exposure to fine particulate matter air pollution and the risk of lung cancer among participants of the

Canadian National Breast Screening Study. *International Journal of Cancer*, ***139***(9), 1958-1966.

Townsley, M. I. (2012). Structure and composition of pulmonary arteries, capillaries, and veins. *Comprehensive Physiology*.

Veshikini, A., Dworkin, S., and Thomson, M. (2015). A soot particle surface reactivitymodel applied to a wide range o flaminar ethylene/air flames. *Combust and Flame*.

Violi, A. (2004). Modeling of soot particle inception in aromatic and aliphatic premixed flames. *Combust. Flame.*, ***139***, 279–287.

Vohr, H.-W. (2016). The Challenge of Predicting the Immunotoxic Potential of Chemicals *Environmental Influences on the Immune System* (pp. 321-340): Springer

Wang, J., Hu, M., Cheng, X., Christakos, G., and Zhao, Y. (2013). Estimation of Citywide Air Pollution in Beijing. *PLoS ONE*, ***8***(1), e53400.

Wang, Z., Li, K., Lambert, P., and Yang, C. (2007). Identification, characterization and quantitation of pyrogenic polycylic aromatic hydrocarbons and other organic compounds in tire fire products. *Journal of Chromatography A*, ***1139***(1), 14-26.

Warnatz, J., Maas, U., and Dibble, R. W. (2006). *Physical and chemical fundamentals, modeling and simulation, experiments, pollutant formation* (4th Edition ed.). Heidelberg: Springer-Verlag Berlin.

Weidemann, E., Andersson, P. L., Bidleman, T., Boman, C., Carlin, D. J., Collina, E., Cormier, S. A., Gouveia-Figueira, S. C., Gullett, B. K., and Johansson, C. (2016). 14th congress of combustion by-products and their health effects—origin, fate, and health effects of combustion-related air pollutants in the coming era of bio-based energy sources. *Environmental Science and Pollution Research*, ***23***(8), 8141-8159.

White, F. (2008). National Institute for Occupational Safety and Health (NIOSH) Prevention through Design (PtD) Workshop Closing Remarks. *Journal of Safety Research*, ***39***(2), 203-204.

Wright, S., Andrews, G., and Sabir, H. (2009). A review of heat exchanger fouling in the context of aircraft air-conditioning systems, and the potential for electrostatic filtering. *Applied Thermal Engineering*, ***29***(13), 2596-2609.

Wyrick, J., Einstein, T., and Bartels, L. (2015). Chemical insight from density functional modeling of molecular adsorption: Tracking the bonding and diffusion of anthracene derivatives on Cu (111) with molecular orbitals. *The Journal of Chemical Physics*, ***142***(10), 101907.

Xi, J., and Zhong, B. J. (2006). Soot in diesel combustion systems. *Chemical Engineering & Technology, **29***(6), 665-673.

Yapp, E., and Kraft, M. (2013). Model of Particle Formation. *Modelling Soot Formation*.

Yu, M., Zheng, X., Witschi, H., and Pinkerton, K. E. (2002). The role of interleukin-6 in pulmonary inflammation and injury induced by exposure to environmental air pollutants. *Toxicological Sciences, **68***(2), 488-497.

Zhang, Q., Thomsona, J., Guob, H., Liub, F., and Smallwood, G. (2009). A numerical study of soot aggregate formation in a laminar coflow diffusion flame. *Combustion and Flame, **156***(3), 697-705.

Zhang, Z., Lina, L., and Wang, L. (2010). Atmospheric oxidation mechanism of naphthalene initiated by OH radical. A theoretical study. *Phys. Chem., **14***, 2645–2650.

APPENDICES

Appendix 1: A sample of SEM micrograph from tyre burning

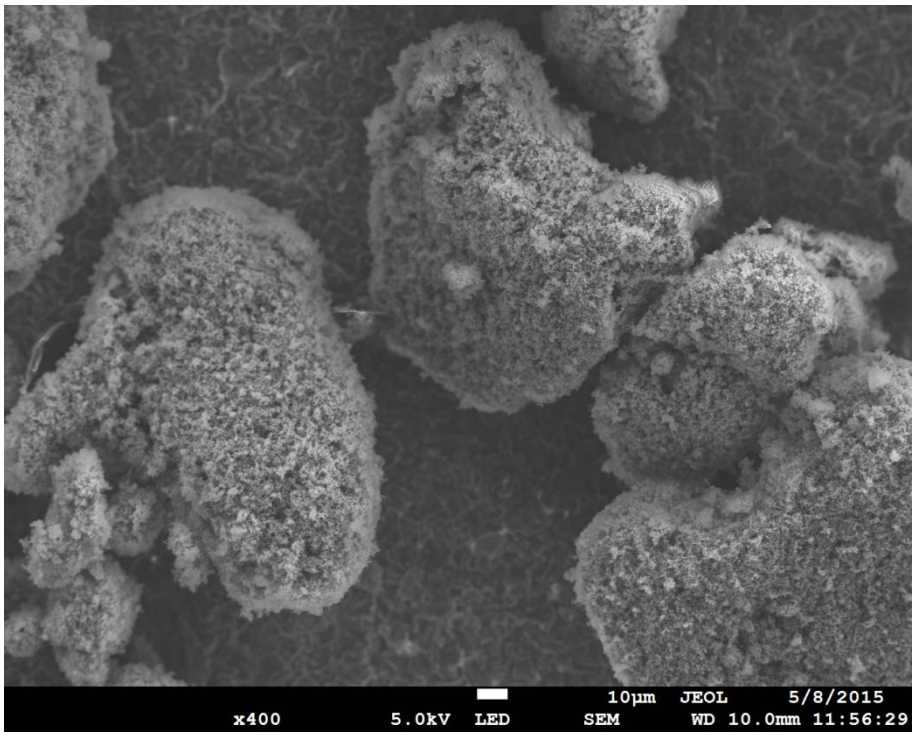

Appendix 2A: MS-Fragmentation pattern for benzene

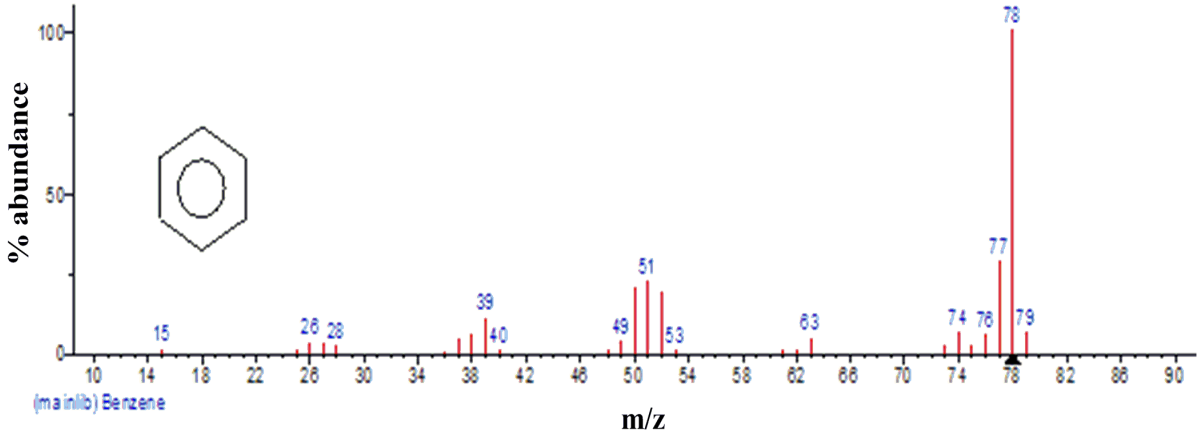

Appendix 2B: MS-Fragmentation pattern for fluorene

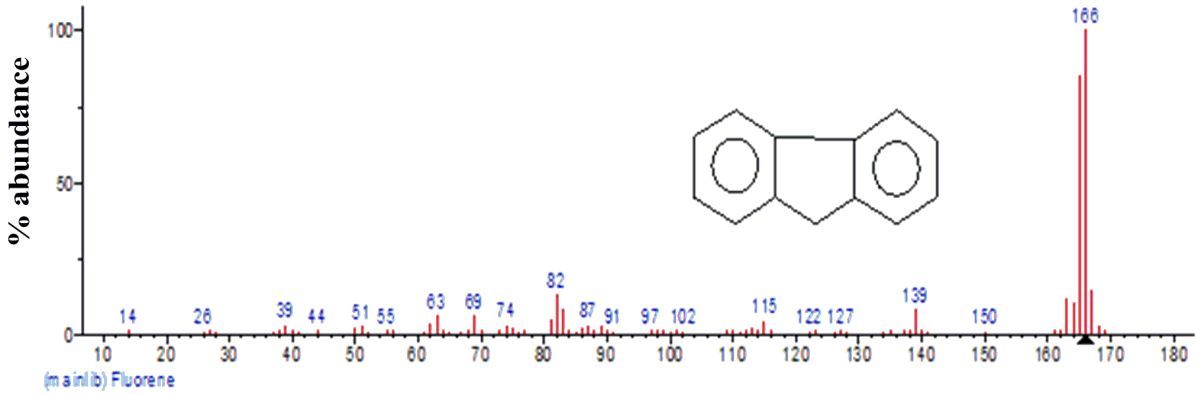

m/z

Appendix 2C: MS-Fragmentation pattern for anthracene

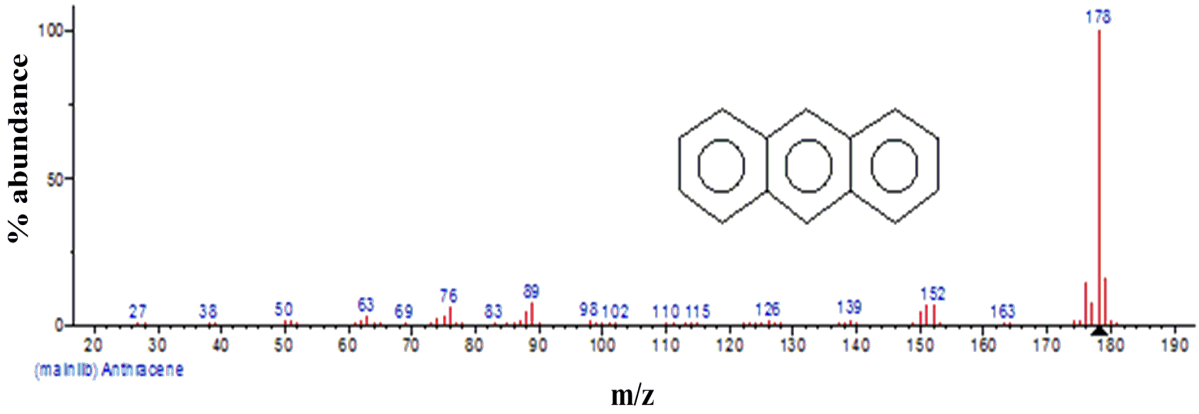

Appendix 2D: MS-Fragmentation pattern for fluoranthene

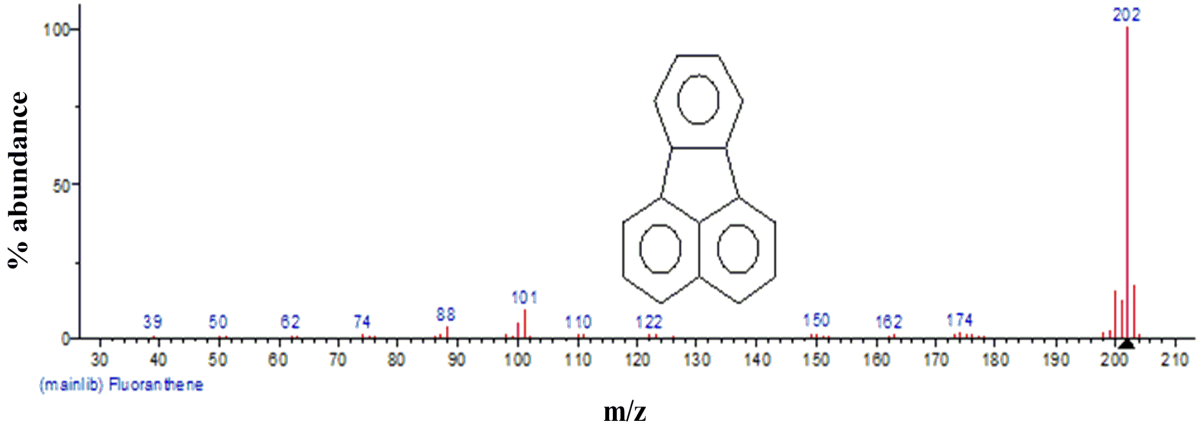

Appendix 2E: MS-Fragmentation pattern for benzo[a]pyrene

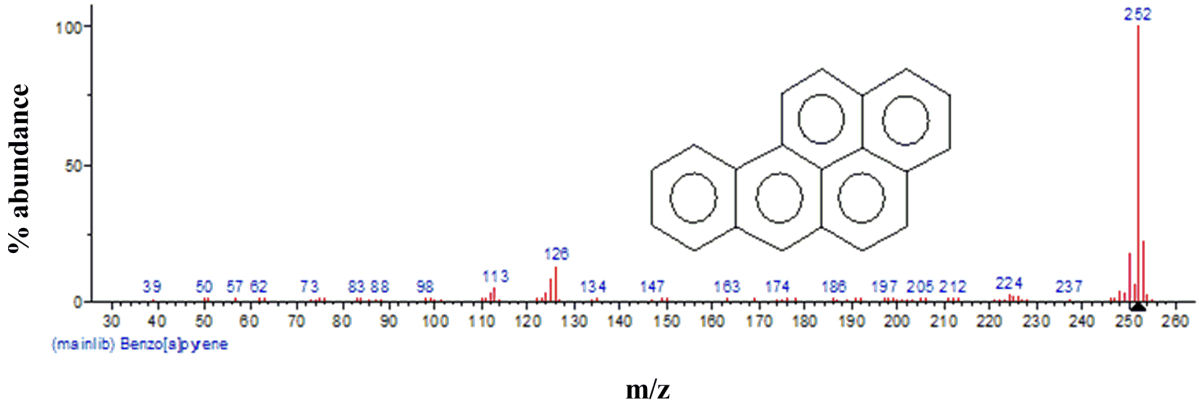

Appendix 3: Thermochemistry output file for optimization of isobenzofuran-1,3-dione

---

- Thermochemistry -

Temperature 298.150 Kelvin. Pressure 1.00000 Atm.

Atom 1 has atomic number 6 and mass 12.00000

Atom 2 has atomic number 6 and mass 12.00000

Atom 3 has atomic number 6 and mass 12.00000

Atom 4 has atomic number 6 and mass 12.00000

Atom 5 has atomic number 6 and mass 12.00000

Atom 6 has atomic number 6 and mass 12.00000

Atom 7 has atomic number 1 and mass 1.00783

Atom 8 has atomic number 1 and mass 1.00783

Atom 9 has atomic number 1 and mass 1.00783

Atom 10 has atomic number 1 and mass 1.00783

Atom 11 has atomic number 6 and mass 12.00000

Atom 12 has atomic number 8 and mass 15.99491

Molecular mass: 104.02621 amu.

Principal axes and moments of inertia in atomic units:

	1	2	3
EIGENVALUES --	324.87295	1034.58108	1359.45403
X	0.00000	0.00000	1.00000
Y	0.00000	1.00000	0.00000
Z	1.00000	0.00000	0.00000

This molecule is an asymmetric top.

Rotational symmetry number 2.

Rotational temperatures (Kelvin) 0.26661 0.08372 0.06371

Rotational constants (GHZ): 5.55522 1.74442 1.32755

Zero-point vibrational energy 222969.3 (Joules/Mol)

53.29093 (Kcal/Mol)

Warning -- explicit consideration of 7 degrees of freedom as

vibrations may cause significant error

Vibrational temperatures: 170.61 382.04 489.34 607.79 741.76

(Kelvin)	843.66	882.48	1028.62	1040.85	1070.48
	1115.41	1251.87	1348.67	1412.00	1445.09
	1450.39	1543.70	1628.26	1675.86	1821.52
	2025.97	2080.07	2109.97	2318.05	2336.81
	2796.25	4479.95	4497.30	4517.97	4521.30

Zero-point correction= 0.084925 (Hartree/Particle)
Thermal correction to Energy= 0.090834
Thermal correction to Enthalpy= 0.091779
Thermal correction to Gibbs Free Energy= 0.055516
Sum of electronic and zero-point Energies= -342.280263
Sum of electronic and thermal Energies= -342.274353
Sum of electronic and thermal Enthalpies= -342.273409
Sum of electronic and thermal Free Energies= -342.309671

	E (Thermal)	CV	S
	KCal/Mol	Cal/Mol-Kelvin	Cal/Mol-Kelvin
Total	56.999	22.430	76.320
Electronic	0.000	0.000	0.000
Translational	0.889	2.981	39.836
Rotational	0.889	2.981	26.238
Vibrational	55.222	16.469	10.246

Appendix 4A: **2**-D electron density contour map for fluoranthene predicted using Chemissian

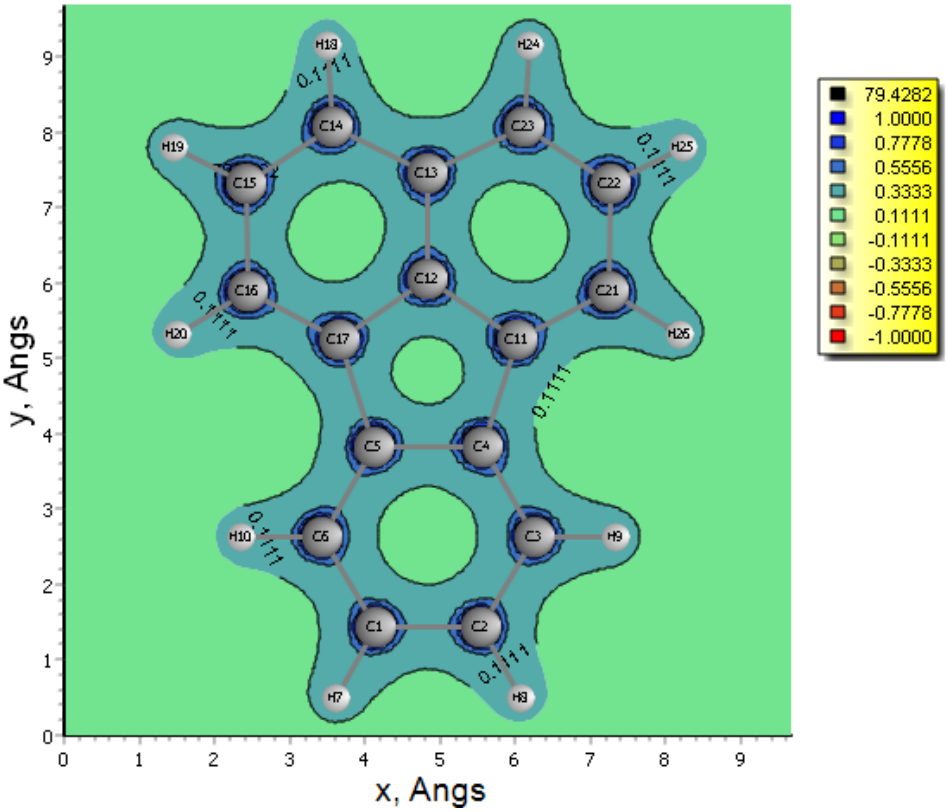

Appendix 4B: HOMO-LUMO band gap for fluoranthene determined using Chemissian

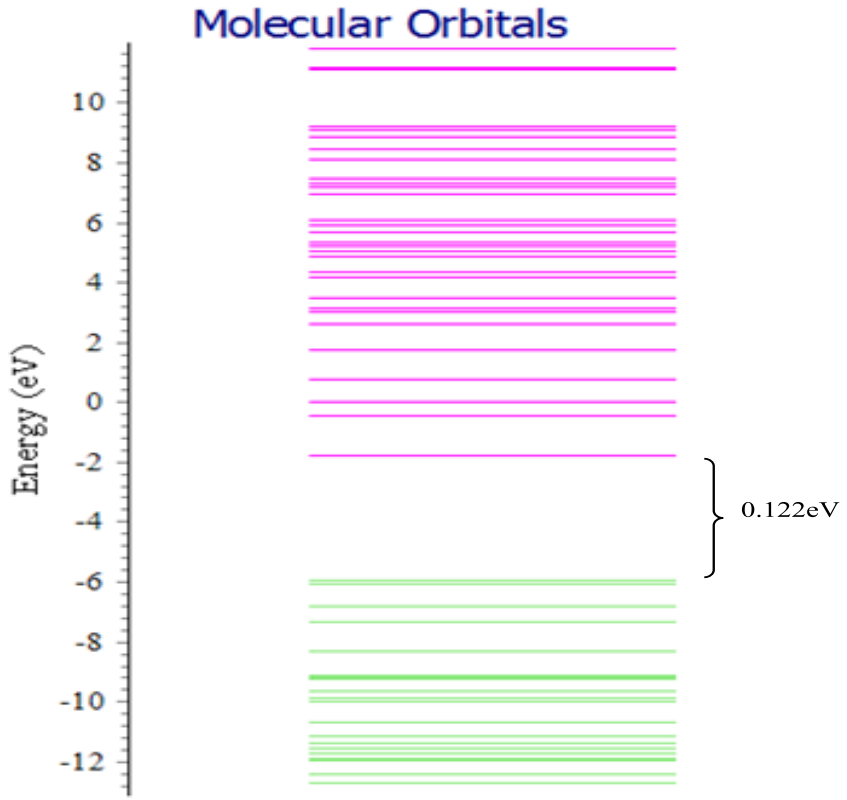

Appendix 5: Albino mice in the cage for soot/smoke exposure